

Chapter II.1

Introduction to radio frequency engineering

Andrea Mostacci

Sapienza University of Rome, Italy

RF engineering in particle accelerators is a multidisciplinary field that combines principles of electromagnetism, RF technology, control systems, and beam physics to ensure the efficient and reliable acceleration of charged particles for various scientific and industrial applications. The aim of this chapter is to review the electromagnetic field theory behind the practice discussed in the following RF engineering section. Starting from Maxwell's equation in vacuum and their solution, we discuss the most commonly used boundary conditions. We review the general boundary value problem to show the properties of electromagnetic fields in cylindrical metallic waveguides. We discuss as well examples relevant for particle accelerator technology.

Radio frequency (RF) engineering applied to particle accelerators involves the design, implementation, and optimization of RF systems and components used in accelerating charged particles to high energies within the accelerator. Particle accelerators are essential tools in various scientific and industrial applications, including high-energy physics research, medical treatment, and material science.

There are several key aspects of RF engineering in the context of modern particle accelerators. For instance, RF cavities, or resonators, are crucial components in particle accelerators. These structures use RF fields to accelerate charged particles. The design of these cavities is a critical aspect of RF engineering, involving considerations such as the frequency of the RF field, the shape of the cavity, and the RF power requirements. RF cavities need to be conditioned to handle the high RF power levels, ranging from few to few tens of MW; such process involves gradually increasing the power levels applied to the RF structure while monitoring and managing various parameters to prevent damage and achieve stable operation.

RF power sources provide the necessary energy to generate the RF fields within the cavities. RF engineers work on designing and optimizing the power sources to ensure efficient and reliable acceleration of particles. RF power is typically distributed with waveguides optimised to minimise losses. Particle accelerators often require high-power RF amplifiers to boost the signal strength. RF engineers focus on developing and maintaining these amplifiers to meet the specific needs of the accelerator.

RF control systems play a vital role in managing and adjusting the RF fields within the accelerator. RF engineers develop sophisticated control systems to ensure precise control over the acceleration process, including feedback mechanisms to maintain stability. The so called low (power) level systems use the most advanced concepts in analog electronics and signal processing to acquire and manipulate

This chapter should be cited as: Introduction to radio frequency engineering, A. Mostacci, DOI: [10.23730/CYRSP-2024-003.733](https://doi.org/10.23730/CYRSP-2024-003.733), in: Proceedings of the Joint Universities Accelerator School (JUAS): Courses and exercises, E. Métral (ed.), CERN Yellow Reports: School Proceedings, CERN-2024-003, DOI: [10.23730/CYRSP-2024-003](https://doi.org/10.23730/CYRSP-2024-003), p. 733.
© CERN, 2024. Published by CERN under the [Creative Commons Attribution 4.0 license](https://creativecommons.org/licenses/by/4.0/).

signals and use them in accelerator controls. Also analog/digital conversion, and thus digital electronics, is becoming increasingly important in the control of modern accelerators.

RF engineers also contribute to the development of diagnostic systems that monitor and analyze the performance of RF components. This includes measuring RF fields, beam characteristics, and overall accelerator performance. In this context analog and digital electronics are used together.

In recent years, RF engineering has played a role in exploring and developing advanced accelerator concepts, such as plasma-based accelerators or novel RF structures, which aim to push the limits of current accelerator technologies.

Lastly, RF engineering is closely tied to the overall beam dynamics of particle accelerators. Engineers work on optimizing the RF parameters to control the trajectory, energy, and focusing of the particle beams.

RF engineering relies on electromagnetic field theory which is a discipline concerned with the study of charges, at rest and in motion, which produce currents and electro-magnetic fields. Nowadays electromagnetic field theory has become indispensable to the understanding, design, and operation of many practical systems using antennas, scattering, microwave circuits and devices, radio-frequency and optical communications, wireless communications, broadcasting, geosciences and remote sensing, radar, radio astronomy, quantum electronics, solid-state circuits and devices, electromechanical energy conversion, and even computers. Circuit theory is a special case of electromagnetic theory, and it is valid when the physical dimensions of the circuit are small compared to the wavelength. Circuit concepts, which deal primarily with lumped elements, must be modified to include distributed elements and coupling phenomena in studies of advanced systems. For example, signal propagation, distortion, and coupling in strip lines used in the design of sophisticated systems (such as computers and electronic packages of integrated circuits as well as in particle beam diagnostics) can be properly accounted for only by understanding the electromagnetic field interactions associated with them.

The study of electromagnetics includes both theoretical and applied concepts. The theoretical concepts are described by a set of basic laws formulated primarily through experiments conducted during the nineteenth century by many scientists—Faraday, Ampere, Gauss, Lenz, Coulomb, Volta, and others. Although Maxwell had come up with 20 equations with 20 variables, it was Heaviside and Hertz that independently put them into a consistent and compact vector form. Both Heaviside and Hertz named them in honour of Maxwell, and today they are the widely acclaimed Maxwell's equations [1]. The applied concepts of electromagnetics, which will be discussed in Section II.1.1, are formulated by applying the theoretical concepts to the design and operation of practical systems.

In this chapter, we will review Maxwell's differential equations, describe the relations between electromagnetic field and circuit theories, derive the boundary conditions associated with electric and magnetic field behaviour across interfaces, relate power and energy concepts for electromagnetic field and circuit theories, and apply all these equations, relations, conditions, concepts, and theories to the study of time-harmonic fields. We will review free space plane wave but the main focus is the solution of Maxwell's equations in closed metallic structures which are of paramount importance in the technology of particle accelerators.

II.1.1 Maxwell's equations

The differential form of Maxwell's equations is the most widely used representation to solve boundary-value electromagnetic problems. It is used to describe and relate the field vectors, current densities, and charge densities at any point in space at any time. For these expressions to be valid, it is assumed that the field vectors are single-valued, bounded, continuous functions of position and time and exhibit continuous derivatives [1].

II.1.1.1 Differential form of Maxwell's equations in vacuum

In vacuum, the electric field \vec{E} (V/m) and the magnetic flux density \vec{B} (Wb/m²) are related to the sources, i.e. the source electric charge density ρ (C/m³) and the source current density \vec{J} (A/m²), by the Maxwell's equations, see Chapter I.1:

$$1. \nabla \cdot \vec{E} = \frac{\rho}{\varepsilon_0}, \quad 2. \nabla \cdot \vec{B} = 0, \quad 3. \nabla \times \vec{E} = -\frac{\partial \vec{B}}{\partial t}, \quad 4. \nabla \times \vec{B} = \mu_0 \vec{J} + \mu_0 \varepsilon_0 \frac{\partial \vec{E}}{\partial t}, \quad (\text{II.1.1})$$

where $\mu_0 = 4\pi \cdot 10^{-7}$ (H/m) is the magnetic constant (also called permeability of the free space) and where $\varepsilon_0 = 8.8542 \cdot 10^{-12}$ (F/m) is the electric constant (also called permittivity of the free space). We are therefore adopting SI units (Units of the International System) through all the chapter.

The physical meaning of the Maxwell's equations can be better understood by recalling the meaning of the divergence ($\nabla \cdot \dots$) and curl ($\nabla \times \dots$) differential operators for the field lines. For any vector field \vec{C} , the scalar differential equation $\nabla \cdot \vec{C} = a$ means that the sources (wells) of the field lines of \vec{C} are the positions where the scalar quantity a is positive (negative). Instead for any vector fields \vec{C} and \vec{G} , the vector differential equations $\nabla \times \vec{C} = \vec{G}$ means that the field lines of \vec{C} and \vec{G} are linked together. Therefore, according to Maxwell's equations II.1.1, the field lines of \vec{E} and \vec{B} are as shown in Fig. II.1.1.

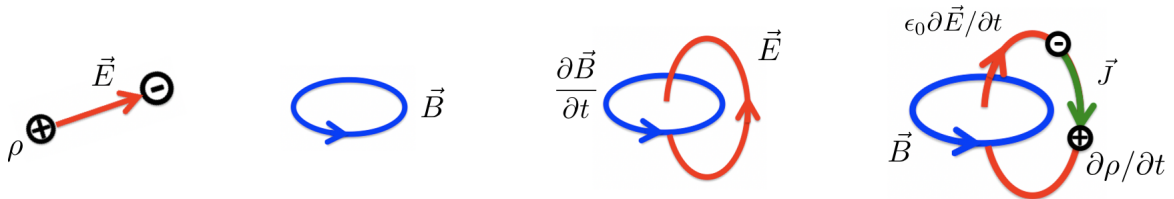


Fig. II.1.1: \vec{E} and \vec{B} field lines according to Maxwell's equations II.1.1.

Since for any vector function $\nabla \cdot (\nabla \times \dots) = 0$, from 4th Maxwell's equation one can write that

$$\nabla \cdot \left(\nabla \times \vec{B} \right) = \mu_0 \nabla \cdot \left(\vec{J} + \varepsilon_0 \frac{\partial \vec{E}}{\partial t} \right) = 0. \quad (\text{II.1.2})$$

Therefore the current density always has closed field lines: the current, due to the flow of charges (i.e. \vec{J}), is closed by the displacement current (i.e. $\varepsilon_0 \partial \vec{E} / \partial t$). By using the 1st Maxwell's equation II.1.1 in Eq. II.1.2, one can prove that at any given position the source (well) of \vec{J} is the decrease (increase) of

charge with time, i.e. the so-called continuity equation for the current density

$$\nabla \cdot \vec{J} + \frac{\partial \rho}{\partial t} = 0, \quad (\text{II.1.3})$$

which is simply the mathematical expression of the electric charge conservation.

In the case of time independent fields $\partial \dots / \partial t = 0$ the continuity equation states that $\nabla \cdot \vec{J} = 0$, the current density always has closed field lines and the flux of \vec{J} (i.e. the current) on any closed surface is always null. Therefore if the charges are moving in a conductor, the amount of charge flowing in any cross section S of the conductor per unit time, i.e. the current $I = \int_S \vec{J} \cdot d\vec{S}$ is constant. An electric network is a closed conductor in which the current flows. $\nabla \cdot \vec{J} = 0$ and Ohm's law, when applied to electric networks, are known as Kirchhoff's laws. The static limit for electric networks is called lumped element model.

The lumped element model for electric networks is used also when the typical time of the field variation is negligible with respect to the time needed by the light to travel along the network ($\partial \dots / \partial t \approx 0$). In this case, one always assumes the existence of electric current I and at any time instant the Kirchhoff laws are valid.

The 3rd Maxwell's equation II.1.1 in the static limit imposes that the \vec{E} field is conservative and thus the energy gain of a charge in closed circuit is zero. This is the fundamental reason why it is not possible to have static circular accelerators; in any circular accelerator the energy of charged particles is changed by using time varying RF \vec{E} fields such that $\nabla \times \vec{E} \neq 0$.

In the static limit, \vec{E} and \vec{B} are decoupled. In the early days of accelerator history, electrostatics played a major role (see for instance Cockcroft–Walton accelerators). The fundamental equations of electrostatics are

$$\nabla \times \vec{E} = 0 \quad \rightarrow \quad \vec{E} = -\nabla V \quad \rightarrow \quad \nabla^2 V = -\frac{\rho}{\epsilon_0}, \quad (\text{II.1.4})$$

being V the scalar electric potential. The last equation for V is called Poisson equation for electrostatics and the Laplace equation is the corresponding homogeneous one, i.e. $\nabla^2 V = 0$.

II.1.1.2 Generalised Maxwell's equations

In the most general case, Maxwell's equations are written with the addition of auxiliary fields to account for the polarisation and magnetisation of matter, namely the electric flux density \vec{D} (C/m²) and the magnetic field \vec{H} (A/m), see Chapter I.1:

$$1. \nabla \cdot \vec{D} = \rho, \quad 2. \nabla \cdot \vec{B} = \rho_m, \quad 3. \nabla \times \vec{E} = -\vec{J}_m - \frac{\partial \vec{B}}{\partial t}, \quad 4. \nabla \times \vec{H} = \vec{J} + \vec{J}_c + \frac{\partial \vec{D}}{\partial t}. \quad (\text{II.1.5})$$

\vec{J}_c is the conduction electric current density (A/m²) accounting for charges moving inside conductors, following the microscopic Ohm's law. Two additional source terms are present, namely the magnetic current density \vec{J}_m (V/m²) and the magnetic charge density ρ_m (Wb/m³) [1]. The continuity equation for $\vec{J} + \vec{J}_c$ can be obviously derived from 4th Maxwell's equation II.1.5, following the same reasoning used to derive Eq. II.1.3.

The electric displacement current $\partial\vec{D}/\partial t$ was introduced by Maxwell to complete Ampere's law for statics. For free space, the displaced current was viewed as a motion of bound charges moving in "ether" an ideal weightless fluid pervading all space. Since ether proved to be undetectable and its concept was not totally reasonable with the special theory of relativity, it has since been disregarded. Instead, for dielectrics, part of the displacement current density has been viewed as a motion of bound charges creating a true current. Because of this, it is convenient to consider, even in free space, the $\partial\vec{D}/\partial t$ term as a displacement current density.

Because of symmetry, the magnetic current density \vec{J}_m and the magnetic charge density ρ_m have been introduced and sometimes the $\partial\vec{B}/\partial t$ is referred to as magnetic displacement current density. Although we have been accustomed to viewing magnetic charges and source magnetic current densities as not being physically realisable, they have been introduced to balance Maxwell's equations [1]. Equivalent magnetic charges and currents are commonly used in many RF engineering problems, both for open space propagation (e.g. with antennas) and for fields propagating in closed structures (e.g. in waveguides). In addition, source magnetic current densities, like source electric current densities, can be considered energy sources that generate fields whose expressions can be written in terms of these current densities.

The solution of some relevant electromagnetic problems can often be aided by the introduction of "equivalent" source electric and magnetic current densities but most of them are outside the scope of this chapter. However, to give the reader a glimpse of the importance and interpretation of the electric and magnetic current densities, let us consider two familiar circuit examples [1].

In Fig. II.1.2 (left), an electric current source is connected in series to a resistor and a parallel-plate capacitor. The electric current density \vec{J} can be viewed as the current source that generates the conduction current density \vec{J}_c through the resistor and the displacement current density $\partial\vec{D}/\partial t$ through the dielectric material of the capacitor. In Fig. II.1.2 (right), a voltage source is connected to a wire that, in turn, is wrapped around a high-permeability magnetic core. The voltage source can be viewed as the source magnetic current density \vec{J}_m that generates the displacement magnetic current density $\partial\vec{B}/\partial t$ through the magnetic material of the core.

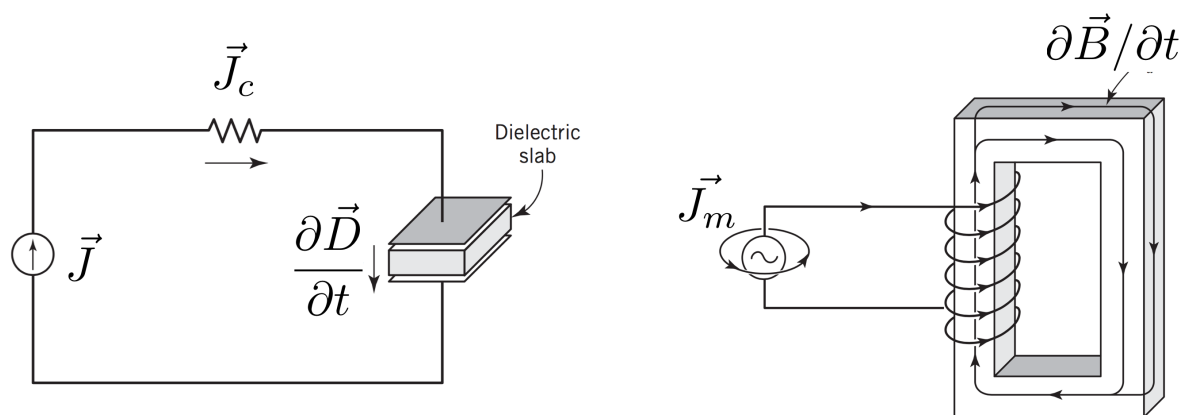


Fig. II.1.2: Circuits with electric (left) and magnetic current densities (right), taken from Ref. [1].

II.1.1.3 Time-harmonic electromagnetic fields

In many practical systems involving electromagnetic waves, the time variations are of sinusoidal form and are referred to as time-harmonic. In general, such time variations can be represented mathematically by $\exp j\omega t$ ($\omega = 2\pi f$ and f being the frequency), and the instantaneous electromagnetic field vectors can be related to their complex forms in a very simple manner. For time-harmonic fields, we can relate the instantaneous fields, current density and charge, e.g. $\vec{E}(\vec{r}, t)$, to their complex form, e.g. $\vec{E}(\vec{r}, \omega)$, by

$$\vec{E}(\vec{r}, t) = \text{Re} \left\{ \vec{E}(\vec{r}, \omega) e^{j\omega t} \right\}. \quad (\text{II.1.6})$$

The complex quantity $\vec{E}(\vec{r}, \omega)$ is called a phasor and it can be defined for any time dependent term of Eq. II.1.5. It represents the complex spatial form and it is only a function of position coordinates. In the following, we will use the same symbol for real and complex vectors; when the meaning will not be obvious, we will write t or ω to make clear which vectors we are using.

The temporal (real) field vector represents instantaneous field vectors; their magnitudes represent peak values that are related to their corresponding root-mean-square (RMS) values by the square root of 2 (peak = $\sqrt{2}$ rms). If the complex spatial quantities can be found, it is then a very simple procedure to find their corresponding instantaneous forms by using relations similar to Eq. II.1.6.

Note that, with phasors, the time evolution of the instantaneous quantities is identical to phase rotation of the complex quantities. Such property is mostly used in modern numerical codes to visualize the evolution of the e.m. quantities with time, after the solution of Maxwell's equations.

When dealing with power and energy we will often be interested in the time average of a quadratic quantity. This can be found very easily for time harmonic fields. For example, the average of the square of the magnitude of an electric field $\vec{E}(\vec{r}, t)$ is

$$\left\langle \left| \vec{E}(\vec{r}, t) \right|^2 \right\rangle_T = \frac{1}{T} \int_0^T \vec{E}(\vec{r}, t) \cdot \vec{E}(\vec{r}, t) = \dots = \frac{1}{2} \vec{E}(\vec{r}, \omega) \cdot \vec{E}(\vec{r}, \omega)^* = \left| \vec{E}_{RMS}(\vec{r}, \omega) \right|^2. \quad (\text{II.1.7})$$

The field of radio frequency (RF) and microwave engineering generally covers the behavior of time-harmonic fields with frequencies in the range of 100 MHz to 1000 GHz. RF frequencies range from very high frequency (VHF) (30–300 MHz) to ultra high frequency (UHF) (300–3000 MHz), while the term microwave is typically used for frequencies between 3 and 300 GHz, with a corresponding electrical wavelength between $\lambda = 10$ cm and $\lambda = 1$ mm, respectively. Electromagnetic waves with wavelengths on the order of millimeters are often referred to as millimeter waves. Figure II.1.3 shows also the location of the RF and microwave frequency bands in the electromagnetic spectrum.

Table II.1.1 describes the nomenclature of the frequency bands mostly relevant for modern particle accelerators. The frequency spectrum from L band (1–2 GHz) to W band (75–110 GHz) encompasses a range of electronic engineering applications. In the L band, frequencies between 1 and 2 GHz find prevalent use in mobile and satellite communication systems due to their ability to provide reliable data rates over extended distances. Progressing to the higher S band (2–4 GHz), applications extend to radar systems and weather monitoring, benefiting from a balance between data rate and signal propagation characteristics. Moving further up, the C band (4–8 GHz) serves roles in satellite communication, mi-

Table II.1.1: Approximate band designation [2].

		Frequency range		Frequency range
Today accelerators	L band	1–2 GHz	S band	2–4 GHz
	C band	4–8 GHz	X band	8–12 GHz
Near future accelerators	Ku band	12–18 GHz	K band	18–26 GHz
	Ka band	26–40 GHz	Q band	33–50 GHz
	U band	40–60 GHz	V band	50–75 GHz
	E band	60–90 GHz	W band	75–110 GHz

microwave links, and weather radar, striking a balance between atmospheric absorption and signal reliability. The X band (8–12 GHz), known for finer radar resolution, is commonly employed in military and weather radar applications. The Ku band (12–18 GHz) excels in satellite communication for high-data-rate transmission. The K band (18–26 GHz) and Ka band (26–40 GHz) further extend capabilities in communication, radar, and remote sensing applications. As we progress into the millimeter-wave spectrum, the Q band (33–50 GHz), U band (40–60 GHz), V band (50–75 GHz), and W band (75–110 GHz) find applications in plasma heating, millimeter-wave communication, short-range communication systems, point-to-point links, and high-frequency microwave signals, enabling precise sensing and imaging capabilities in various fields. Particle accelerators profit continuously of the technological development driven by all those applications.

As shown in Tab. II.1.1 particle accelerators presently in operation typically use devices with frequencies from L-band to X-band. Higher frequency devices are undergoing a worldwide R&D effort to be used (hopefully) in the next generation accelerators.

Figure II.1.3 shows the electromagnetic spectrum in the interval of interesting for RF engineers [2] from hundreds of kHz up to the optical region, emphasising applications to RF particle accelerators. Structures operating in different frequency ranges require to be built from different materials. Up to the infrared region, devices are typically built in copper which has high conductivity as well as optimal vacuum performances. Higher frequencies result in increasing losses, and dielectric materials are thus preferred.

The range of frequencies used for structures capable of manipulating the beam (through acceleration and/or deflection) is influenced by various competing factors, as discussed in Chapter I.11, for example. One critical factor is the availability of stable, reliable RF power sources in the range of tens of megawatts, as required in modern accelerators. Consequently, the development of accelerators is intricately connected to the RF industry. Figure II.1.3 illustrates the frequencies currently utilised in accelerators (white background). It also highlights (green background) ongoing research and development directions (R&D) that, ideally, will shape the future of next generation particle accelerators.

In Fig. II.1.3, we also report examples of accelerating cavities (see Chapter I.1) working at different frequencies. The oldest one is the cavity of a 1.5 GeV electron positron storage ring (ADONE at National Laboratory of Frascati, Italy, 1965) operating at 8.58 MHz [3]. The one working at 800 MHz is a low beam energy Side Coupled Drift Tube Linac (SCDTL) copper structure [4], shown at the right bottom corner. One example of superconducting cavities is the 1.3 GHz multi-cell cavity from the TESLA linear accelerator at DESY laboratory (Hamburg, Germany) [5]. The 3 GHz cavity is the state-of-the-art of

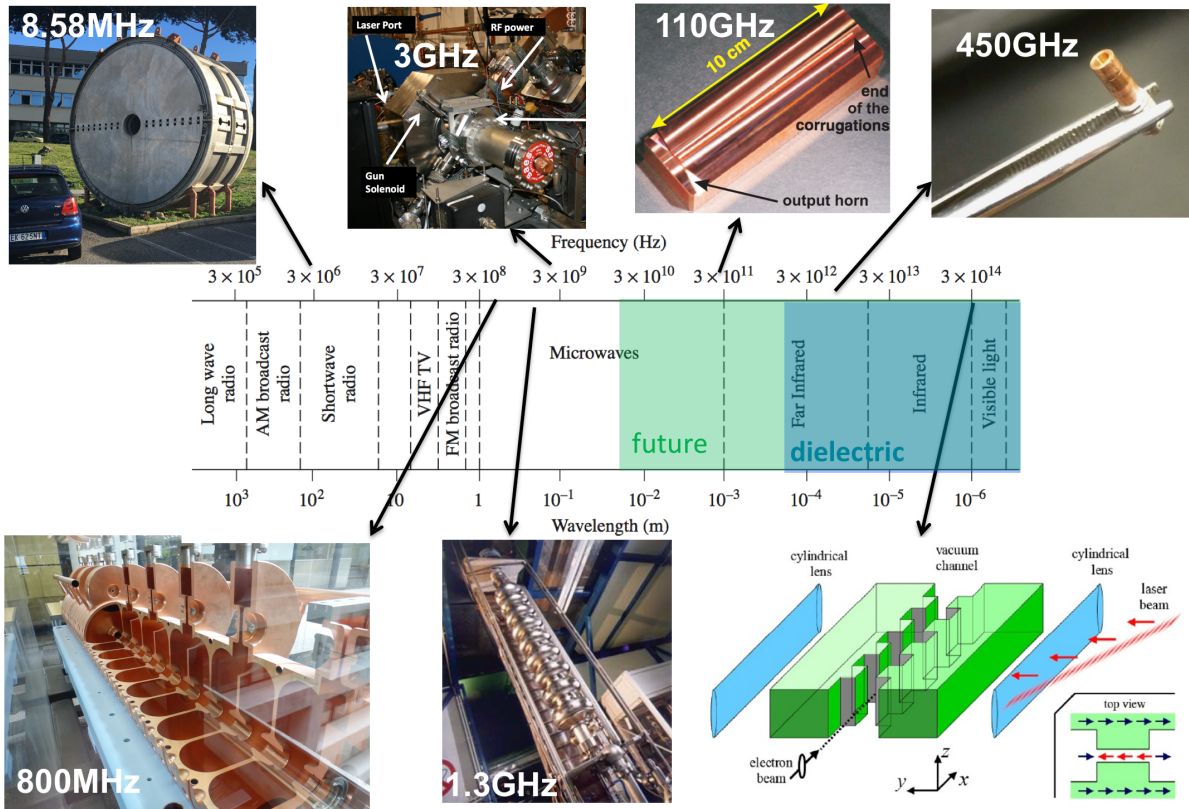


Fig. II.1.3: Modern accelerator devices and their occupancy in the electro-magnetic spectrum.

most of high beam brightness linacs used in modern Free Electron Lasers [6]. Compact copper structure at 110 GHz are presently in the R&D phase [7]. Sub-THz (and THz as well) structures are believed to be of promise for future accelerators and they are being investigated worldwide; Fig. II.1.3 shows an example from Ref. [8]. The high intensity laser fields can not directly accelerate particles in free space, but they can be used to feed a dielectric structure as shown in the Fig. II.1.3 bottom right device [9].

II.1.1.4 Constitutive relations

Materials contain charged particles, and when these materials are subjected to electromagnetic fields, their charged particles interact with the electromagnetic field vectors, producing currents and modifying the electromagnetic wave propagation in these media compared to that in free space. To account on a macroscopic scale for the presence and behavior of these charged particles, without introducing them in a microscopic lattice structure, usually one gives a set of three expressions relating the electromagnetic field vectors. These expressions are referred to as the constitutive relations.

Field equivalence principle [10] suggests that the behaviour of polarized or magnetized materials can be treated as equivalent to free space with the addition of specific sources, namely polarization charges or magnetization currents acting in vacuum (i.e. according to Maxwell's equations II.1.1). This simplifies the mathematical treatment of the interactions between electromagnetic fields and materials.

A more complete discussion of this is given in Chapter I.1 or in modern electromagnetic engineering textbooks, e.g. Ref. [1]. Since the late 1990s a renewed interest has been spurred in the application,

integration, modelling, and optimisation of materials in a plethora of electromagnetic radiation, guiding, and scattering structures. An inclusive name for all these materials is *metamaterials*. It is the class of metamaterials that has captivated the interest and imagination of many leading researchers and practitioners, scientists, and engineers from academia, industry, and government. When electromagnetic waves interact with such surfaces, they result in some very unique and intriguing characteristics and phenomena that can be used, for example, to optimise the performance of antennas, microwave devices, and other electromagnetic wave guiding structures.

Such materials are not so common in accelerator practice, because of practical reasons related to vacuum performances or the presence of high electric field, potentially damaging such materials. In accelerator technology, we deal mainly with high electrical conductivity materials (i.e. electric conductors) when building accelerator devices or high magnetic permeability materials (i.e. ferromagnetic materials) in magnets. Ferrite is used in some devices such as high power phase shifters. Magnetic (perfect) conductors are sometimes used in RF device simulations, but this will be discussed in the context of boundary conditions.

We will limit our analysis to linear, homogeneous, isotropic and stationary media, where one can write

$$\vec{D} = \varepsilon_c \vec{E} \quad \text{with} \quad \varepsilon_c = \varepsilon' - j\varepsilon'' \quad \text{and} \quad \vec{B} = \mu \vec{H} \quad \text{with} \quad \mu = \mu' - j\mu''. \quad (\text{II.1.8})$$

The imaginary part of the complex permeability ε'' (permittivity μ'') account for losses (i.e. heating) due to damping of vibrating dipoles (magnetic currents). Due to the Ohm's law, the current density in the conductor \vec{J}_c is such that

$$\vec{J}_c = \sigma \vec{E}, \quad (\text{II.1.9})$$

with σ the electric conductivity in (S/m) accounting for losses (i.e. heating) due to moving charges colliding with the lattice. The three relations in Eqs. II.1.8 and II.1.9 are referred to as the constitutive relations for time harmonic fields (or in the frequency domain) [1].

Constitutive relations in tensor form are commonly used in electromagnetic engineering when dealing with anisotropic materials, i.e. materials exhibiting different electromagnetic properties in different directions; such an approach is beyond the scope of this work.

II.1.1.5 A solution of Maxwell's equations: the plane waves

Using phasors, Maxwell's equations in differential (and even integral forms) for time-harmonic electromagnetic fields can be written in much simpler forms, since

$$e^{j\omega t} = e^{j2\pi f t} \quad \rightarrow \quad \frac{\partial}{\partial t} \dots = j\omega \dots$$

If the source terms are zero, Eqs. II.1.5 imply that

$$1. \nabla \cdot \vec{D} = 0, \quad 2. \nabla \cdot \vec{B} = 0, \quad 3. \nabla \times \vec{E} = -j\omega\mu\vec{H} \quad 4. \nabla \times \vec{H} = j\omega\varepsilon\vec{E} \quad (\text{II.1.10})$$

which are the general homogeneous Maxwell's equations, provided that

$$\varepsilon = \varepsilon' - j\varepsilon'' - j\frac{\sigma}{\omega} = \varepsilon_r\varepsilon_0(1 - j \tan \delta) \quad \text{being} \quad \tan \delta = \frac{\omega\varepsilon'' + \sigma}{\omega\varepsilon'} \propto \frac{\text{Losses}}{\text{Displacement current}}; \quad (\text{II.1.11})$$

$\tan \delta$ is called loss tangent and ε_r is the relative dielectric constant.

The wave equation for the electric field in vacuum

$$\nabla^2 \vec{E} = \mu_0\varepsilon_0 \frac{\partial^2 \vec{E}}{\partial t^2} \quad \text{becomes} \quad \nabla^2 \vec{E} + \omega^2 \mu\varepsilon \vec{E} = 0 \quad (\text{II.1.12})$$

for a general linear, homogeneous, isotropic and stationary media. The last equation is called the Helmholtz equation and $k = \omega\sqrt{\varepsilon\mu}$ is the propagation constant or wave number (1/m).

The simplest solution is the plane wave, i.e. a wave with a plane wave-front. For instance, if $\vec{E} = E_x \hat{x}$, uniform in \hat{x} and \hat{y} and the medium is lossless

$$\frac{\partial}{\partial x} \dots = \frac{\partial}{\partial y} \dots = 0 \quad \rightarrow \quad \frac{d^2 E_x}{dz^2} + k^2 E_x = 0 \quad \rightarrow \quad E_x(z, \omega) = E^+ e^{-jkz} + E^- e^{jkz}. \quad (\text{II.1.13})$$

The instantaneous electric field reads

$$E_x(z, t) = \text{Re} \{ E_x(z, \omega) e^{j\omega t} \} = E^+ \cos(\omega t - kz) + E^- \cos(\omega t + kz), \quad (\text{II.1.14})$$

which is a wave moving in the positive and negative \hat{z} -direction.

The velocity at which a fixed phase point on the wave front travels, namely the phase velocity v_p , is such that $\omega t \pm kz$ is constant and thus

$$\text{if } \omega t \pm kz = \text{const}, \quad v_p = \left| \frac{dz}{dt} \right| = \left| \frac{d}{dt} \left(\frac{\omega t \pm \text{const}}{k} \right) \right| = \frac{\omega}{k} = \frac{1}{\sqrt{\varepsilon\mu}}, \quad (\text{II.1.15})$$

which is the speed of light in the medium. The wavelength λ is defined as the distance between two successive maxima (or minima, or any other corresponding reference points) on the wave at a fixed instant of time, i.e.

$$(\omega t - kz) - [\omega t - k(z + \lambda)] = 2\pi, \quad \lambda = \frac{2\pi}{k} = \frac{2\pi v_p}{\omega} = \frac{v_p}{f}.$$

Using Eq. II.1.13 in the 4th Maxwell's equation II.1.10

$$H_x = H_z = 0 \quad H_y = \frac{j}{\omega\mu} \frac{\partial E_x}{\partial z} = \frac{1}{\eta} (E^+ e^{-jkz} - E^- e^{jkz}) \quad \text{with} \quad \eta = \frac{\omega\mu}{k} = \sqrt{\frac{\mu}{\varepsilon}} = \frac{1}{\varepsilon v} = \mu v; \quad (\text{II.1.16})$$

η is called intrinsic impedance of the medium and $\eta_0 = \sqrt{\mu_0/\varepsilon_0} = 377\Omega$ is its value for vacuum. Note that the \vec{E} and \vec{H} vectors are orthogonal to each other and orthogonal to the direction of propagation (\vec{k}), i.e.

$$\vec{H} = \frac{1}{\eta} \vec{k} \times \vec{E}; \quad (\text{II.1.17})$$

this is a peculiar property of Transverse Electro-Magnetic (TEM) waves. The ratio between electric and

magnetic field components is an impedance and it is called wave impedance $Z_{\text{TEM}} = \eta$. In optical engineering, in which the wavelength is much shorter than the dimensions of the component, the plane wave solution is very often used, leading to the geometrical optics regime; optical systems can be designed with the theory of geometrical optics.

II.1.1.6 Energy conservation and Poynting theorem

In a volume τ bounded by a closed surface A , the energy of the e.m. field is

$$U = \int_{\tau} \frac{1}{2} \vec{E} \cdot \vec{D} \, d\tau + \int_{\tau} \frac{1}{2} \vec{H} \cdot \vec{B} \, d\tau = \int_{\tau} u_E \, d\tau + \int_{\tau} u_H \, d\tau;$$

u_E (u_H) is the density of electric (magnetic) energy in J/m^3 . Using Maxwell's equations, vector identities and divergence theorem, the rate of decrease of e.m. energy in τ can be written

$$-\frac{dU}{dt} = - \int_{\tau} \left(\vec{E} \cdot \frac{\partial \vec{D}}{\partial t} + \vec{H} \cdot \frac{\partial \vec{B}}{\partial t} \right) d\tau = \int_{\tau} \vec{E} \cdot \vec{J} \, d\tau + \oint_A \vec{S} \cdot d\vec{A}, \quad (\text{II.1.18})$$

where $\vec{S}(\vec{r}, t) = \vec{E}(\vec{r}, t) \times \vec{H}(\vec{r}, t)$ is called Poynting vector with dimensions of W/m^2 . The $\vec{E} \cdot \vec{J}$ term accounts for energy per unit time transferred from electric field to moving charges in τ , namely dissipated power P (Joule effect) in τ , since

$$\vec{J} \cdot \vec{E} \, d\tau = \vec{E} \cdot n e \vec{v} \, d\tau = dq \vec{E} \cdot \vec{v} = d\vec{F} \cdot \vec{v} = dP.$$

Electromagnetic energy flowing through surface A per unit time (exiting from τ), namely the radiated power P_{rad} through A , is taken into account by the surface integral of \vec{S} .

Equation II.1.18 is known as Poynting's theorem, after the physicist J. H. Poynting (1852–1914). It is basically a power balance equation stating that the variation of energy in the volume τ per unit time is due to the power dissipated in τ for Joule effect and power radiated through its boundary A .

If in the volume τ there is free space and there are not charges, applying the divergence theorem, the integral Eq. II.1.18 is very often written in its differential form, that is

$$\nabla \cdot \vec{S} + \frac{\partial u}{\partial t} = 0 \quad \text{being} \quad u = u_E + u_H. \quad (\text{II.1.19})$$

For time-harmonic fields, we can use phasor notation and the Poynting vector reads

$$\vec{S}(\vec{r}, t) = \text{Re} \left\{ \frac{\vec{E}(\vec{r}, \omega) \times \vec{H}(\vec{r}, \omega)^*}{2} \right\} + \text{Re} \left\{ \frac{\vec{E}(\vec{r}, \omega) \times \vec{H}(\vec{r}, \omega) e^{j2\omega t}}{2} \right\}, \quad (\text{II.1.20})$$

where the first term is constant with time and it is the time average over a period T , i.e. $\langle \vec{S}(\vec{r}, t) \rangle_T$; the second term at the right-hand side (r.h.s.) is oscillating with the double frequency. One can now understand one possible definition of phasor of $\vec{S}(\vec{r}, t)$ which is

$$\vec{S}(\vec{r}, \omega) = \frac{\vec{E}(\vec{r}, \omega) \times \vec{H}(\vec{r}, \omega)^*}{2}. \quad (\text{II.1.21})$$

Such definition is used in state-of-the-art electromagnetic codes, which are nowadays extensively used for the design RF devices of particle accelerators. The real part of $\vec{S}(\vec{r}, \omega)$ accounts for the active power and it is important to compute the net transfer of energy in a given direction over time. Its imaginary part is related to the reactive power in the volume τ which does not contribute to the net power transfer but it must be taken into account when doing energy balance.

II.1.1.6.1 Analogy among transport phenomena descriptions

To better understand the physical meaning of the Poynting vector $\vec{S}(\vec{r}, t)$, let's consider plane waves; because of Eq. II.1.17, one can write

$$\vec{S} = \frac{1}{\eta} \vec{E} \times (\vec{k} \times \vec{E}) = \frac{1}{\eta} \vec{E} \cdot \vec{E} \hat{k} = \varepsilon |\vec{E}|^2 \vec{v} = \left(\frac{\varepsilon |\vec{E}|^2}{2} + \frac{\mu |\vec{H}|^2}{2} \right) \vec{v} = (u_E + u_H) \vec{v} = u \vec{v}. \quad (\text{II.1.22})$$

Therefore the propagation of electromagnetic energy is described by $\vec{S}(\vec{r}, t)$ which is the product of the volume density of electromagnetic energy times its velocity of propagation. Energy per unit time is conserved and thus $\vec{S}(\vec{r}, t)$ must satisfy Eq. II.1.19. The quantity of electromagnetic energy per unit time passing through a generic surface A is computed by the flux of $\vec{S}(\vec{r}, t)$ on A . Thus

$$\vec{S} = u \vec{v} \left(\frac{W}{m^2} \right) \quad \text{with} \quad \nabla \cdot \vec{S} + \frac{\partial u}{\partial t} = 0 \quad \text{being} \quad P_{\text{rad}} = \int_A \vec{S} \cdot d\vec{A} = \frac{dU}{dt} \quad \text{through } A \quad (\text{II.1.23})$$

where dU/dt is called P_{rad} as radiated power (measured in W).

In various branches of physics, it is customary to describe transport processes through the utilisation of a vectors being the product of the volume density of the quantity being transported and its velocity.

For instance, when dealing with the motion of charges, one defines the current density \vec{J} as the product of the volume density of the moving charges ρ_{mob} and their speed \vec{v} . The total charge must be conserved at any time; therefore \vec{J} and ρ_{mob} satisfy an equation mathematically identical to Eq. II.1.19, which is often called the continuity equation for charges. Indeed

$$\vec{J} = \rho_{\text{mob}} \vec{v} \left(\frac{A}{m^2} \right) \quad \text{with} \quad \nabla \cdot \vec{J} + \frac{\partial \rho_{\text{mob}}}{\partial t} = 0 \quad \text{being} \quad I = \int_A \vec{J} \cdot d\vec{A} = \frac{dQ}{dt} \quad \text{through } A \quad (\text{II.1.24})$$

where the current, i.e. the charge per unit time passing through a surface A , is the flux of \vec{J} .

In fluid dynamics, the continuity equation refers to the conservation of mass, which states that the mass flow rate into a control volume must equal the mass flow rate out of that volume. Usually one introduces the mass flux density \vec{J}_m as the product of the volume mass density ρ_m and the speed \vec{v} . In formulae:

$$\vec{J}_m = \rho_m \vec{v} \left(\frac{kg/s}{m^2} \right) \quad \text{with} \quad \nabla \cdot \vec{J}_m + \frac{\partial \rho_m}{\partial t} = 0 \quad \text{being} \quad \int_A \vec{J}_m \cdot d\vec{A} = \frac{dm}{dt} \quad \text{through } A; \quad (\text{II.1.25})$$

that is the mass moving through a surface per unit time is the flux of \vec{J}_m .

Continuity equation states that the rate of change of a certain quantity within a specified volume is equal to the net flow of that quantity into or out of the volume. In various contexts, the continuity equation takes different forms, but they all express the same underlying principle of conservation. Equation II.1.19 is thus the continuity equation for electromagnetic energy.

For the electromagnetic energy, in a more general form, i.e. including also the energy transferred from the wave to moving charges (Joule effect), Eq. II.1.19 becomes

$$\nabla \cdot \vec{S} + \frac{\partial u}{\partial t} = -\vec{E} \cdot \vec{J}. \quad (\text{II.1.26})$$

The left-hand side of the equation represents the change in energy density within the specified volume due to the flow of electromagnetic energy. The r.h.s. represents the rate at which work is done on the charges within the volume by the electromagnetic field.

In essence, Eq. II.1.26 is a form of continuity equation for electromagnetic energy. It describes how the energy within a given volume changes over time due to the flow of electromagnetic energy into or out of the volume, similar to how a continuity equation describes the conservation of mass or charge within a system.

II.1.2 Boundary conditions

We have seen that Maxwell's equations assume that the field vectors are single-valued, bounded, continuous functions of position and time and exhibit continuous derivatives. Field vectors associated with electromagnetic waves possess these characteristics except where there exist abrupt changes in charge and current densities. Discontinuous distributions of charges and currents usually occur at interfaces between media where there are discrete changes in the electrical parameters across the interface. The variations of the field vectors across such boundaries (interfaces) are related to the discontinuous distributions of charges and currents by what are usually referred to as the boundary conditions. Thus a complete description of the field vectors at any point (including discontinuities) at any time requires not only Maxwell's equations in differential form but also the associated boundary conditions [1].

A detailed description can be found in Chapter I.1 or in Refs. [1, 2]. In this chapter we limit ourselves to the general results and discuss a couple of examples common in RF engineering for accelerators.

Consider a plane interface between two media, as shown in Fig. II.1.4 where $(\vec{J}_{m,S}, \vec{J}_S)$ and $(\rho_{m,S}, \rho_S)$ are the magnetic and electric linear (per meter) current and surface (per square meter) charge densities, respectively.

Maxwell's equations in integral form can be used to deduce conditions involving the normal and tangential fields at this interface. In the most general form, i.e. electric and magnetic sources (charges and current densities) are present along the interface between the two media with neither one being a perfect conductor, the boundary conditions on the tangential and normal components of the fields can be

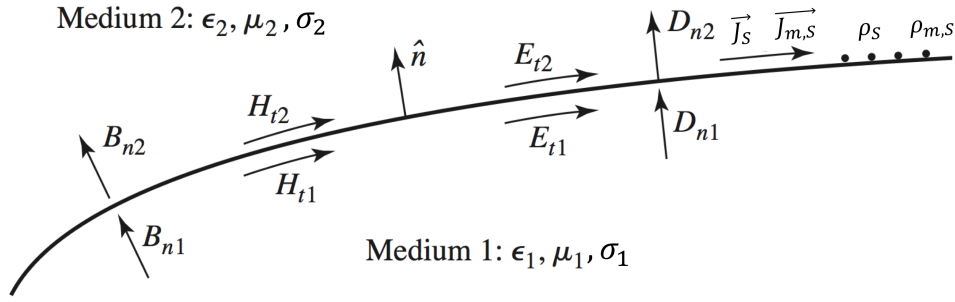


Fig. II.1.4: Fields, currents, and surface charge at a general interface between two media (picture adapted from Ref. [2]).

written as

$$-\hat{n} \times (\vec{E}_2 - \vec{E}_1) = \vec{J}_{m,S}, \quad \hat{n} \times (\vec{H}_2 - \vec{H}_1) = \vec{J}_S, \quad \hat{n} \cdot (\vec{D}_2 - \vec{D}_1) = \rho_S, \quad \hat{n} \cdot (\vec{B}_2 - \vec{B}_1) = \rho_{m,S}. \quad (\text{II.1.27})$$

The three most common cases in practice are finite conductivity media with no sources on the boundaries and the perfect electric and magnetic conductor cases.

In the first case, at the interface with two finite conductivity media, no charge or surface current densities will ordinarily exist; thus Eqs. II.1.27 become

$$\hat{n} \times \vec{E}_1 = \hat{n} \times \vec{E}_2, \quad \hat{n} \times \vec{H}_1 = \hat{n} \times \vec{H}_2, \quad \hat{n} \cdot \vec{D}_1 = \hat{n} \cdot \vec{D}_2, \quad \hat{n} \cdot \vec{B}_1 = \hat{n} \cdot \vec{B}_2. \quad (\text{II.1.28})$$

In words, these equations state that the normal components of \vec{D} and \vec{B} are continuous across the interface, and the tangential components of \vec{E} and \vec{H} are continuous across the interface. Because Maxwell's equations are not all linearly independent, the six boundary conditions contained in the above equations are not all linearly independent. Thus, the enforcement of the conditions for the four tangential field components, for example, will automatically force the satisfaction of the equations for the continuity of the normal components.

Many problems in microwave engineering involve boundaries with good conductors (e.g., metals), which can often be assumed as lossless ($\sigma \rightarrow \infty$). In this case of a perfect conductor, all field components must be zero inside the conducting region (medium 1 if we assume the notation of Fig. II.1.4). Assuming $\sigma_1 \rightarrow \infty$, $\sigma_2 < \infty$, $\vec{J}_{m,S} = 0$ and $\rho_{m,S} = 0$ in Fig. II.1.4, we get

$$\hat{n} \times \vec{E} = 0, \quad \hat{n} \times \vec{H} = \vec{J}_S, \quad \hat{n} \cdot \vec{D} = \rho_S, \quad \hat{n} \cdot \vec{B} = 0, \quad (\text{II.1.29})$$

since now the electromagnetic field exists only in medium 2. A picture of the field at the perfect conductor's surface is given in the left plot of Fig. II.1.5. Such a boundary is sometimes called Perfect Electric Conductor (PEC) and it is also known as an *electric wall* because the tangential components of \vec{E} are “shorted out,” as seen from the first of Eqs. II.1.29, and it must vanish at the surface of the conductor.

Dual to the preceding boundary condition is the magnetic wall boundary condition, where the

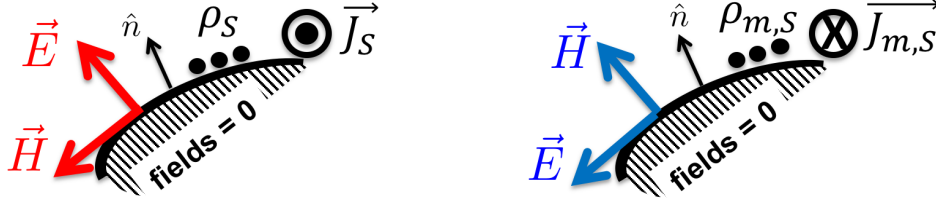


Fig. II.1.5: Fields, surface current and charge for a perfect electric conductor (left picture) and a perfect magnetic one (right picture).

tangential components of \vec{H} must vanish. The magnetic wall condition, then, provides a degree of completeness in our formulation of boundary conditions and is a useful approximation in several cases of practical interest. As shown in the right picture of Fig. II.1.5,

$$\hat{n} \times \vec{E} = -\vec{J}_{m,S}, \quad \hat{n} \times \vec{H} = 0, \quad \hat{n} \cdot \vec{D} = 0, \quad \hat{n} \cdot \vec{B} = \rho_{m,S}. \quad (\text{II.1.30})$$

In general, a magnetic conductor is defined as a material inside of which both time-varying electric and magnetic fields vanish when it is subjected to an electromagnetic field [1]. The tangential components of the magnetic field also vanish next to its surface. In addition, the magnetic charge moves to the surface of the material and creates a magnetic current density that resides on a very thin layer at the surface. Although such materials do not physically exist, they are often used in electromagnetics to develop electrical equivalents that yield the same answers as the actual physical problems. In reality, perfect magnetic conductors can be synthesized approximately over a limited frequency range (band-gap). In the accelerator technology, high μ materials used to increase \vec{B} -field in magnets can be approximated with a Perfect Magnetic Conductor (PMC).

II.1.2.1 Plane waves in lossy media

Electromagnetic waves that travel in lossy media undergo attenuation. In this section we want to discuss the solution for the electric and magnetic fields of uniform plane waves as they travel in lossy media.

Considering the complex permittivity, one can define a γ factor such that

$$j\omega\sqrt{\mu\varepsilon} = \gamma = \alpha + j\beta = j\omega\sqrt{\mu\varepsilon_0\varepsilon_r(1 - j\tan\delta)}, \quad (\text{II.1.31})$$

where α is the attenuation constant and β the phase constant (as in lossless space). Considering a x -polarisation and since E_x is uniform in x and y , Helmholtz equation II.1.12 becomes

$$\frac{d^2 E_x}{dz^2} - \gamma^2 E_x = 0 \quad \text{then} \quad E_x(z, \omega) = E^+ e^{-\gamma z} + E^- e^{\gamma z} \quad \text{being} \quad e^{-\gamma z} = e^{-\alpha z} e^{-j\beta z}. \quad (\text{II.1.32})$$

To resume the time dependence of the \vec{E} field from the phasor, one should take the real part as in

$$\text{Re} \left\{ E^+ e^{-\alpha z} e^{j(\omega t - \beta z)} + \dots \right\} = |E^+| e^{-\alpha z} \cos(\omega t - \beta z + \angle E^+) + \dots \quad (\text{II.1.33})$$

where the ... stands for the regressive wave. The wave phase velocity $v_p = \omega/\beta$ and the wavelength $\lambda = 2\pi/\beta$ are not affected by the losses. E^+ is a complex number of which the modulus contributes to the wave amplitude, while its phase affects the wave initial phase.

From Maxwell's equations one can get the \vec{H} field, which results to be only H_y , i.e.

$$H_y = \frac{j}{\omega\mu} \frac{\partial E_x}{\partial z} = \frac{1}{\eta} (E^+ e^{-j\gamma z} - E^- e^{j\gamma z}) \quad \text{with} \quad \eta = \frac{j\omega\mu}{\gamma} = Z_{\text{TEM}} \quad \text{and} \quad \vec{H} = \frac{1}{\eta} \hat{\beta} \times \vec{E}. \quad (\text{II.1.34})$$

Therefore, a plane wave in a lossy medium is an “attenuated” Transverse Electro-Magnetic (TEM) wave.

For a good electric conductor, when the conduction current σE is much bigger than the displacement current $\omega\epsilon E$, one can write

$$\tan \delta = \frac{\omega\epsilon'' + \sigma}{\omega\epsilon'} \approx \frac{\sigma}{\omega\epsilon_0\epsilon_r}, \quad \gamma \approx (1+j) \sqrt{\frac{\omega\mu\sigma}{2}} \quad \text{with} \quad \delta_S = \frac{1}{\alpha} = \sqrt{\frac{2}{\omega\mu\sigma}} \quad (\text{m})$$

called the skin depth. Therefore the amplitude of a TEM wave travelling in a good conductor will exhibit a behaviour qualitatively shown in Fig. II.1.6, assuming the (infinite) space divided in two parts, one semi-space of vacuum and one of a good conductor. The flat plane interface between the vacuum and a good conductor is placed at $z = 0$; the wave propagating in the positive z -direction has an amplitude E_0 when it impinges on the conductor. According to the first of Eqs. II.1.28, the E -field is continuous at the boundary, then its amplitude is reduced exponentially with z according to Eq. II.1.33. The skin depth δ_S is the inverse of the attenuation constant α ; the linear expansion of the exponential for small z intersects the horizontal axis at $z = \delta_S$, allowing an estimations of the field penetration inside the conductor. The right-hand picture underlines that the wave-length λ is not changing while entering the conductor.

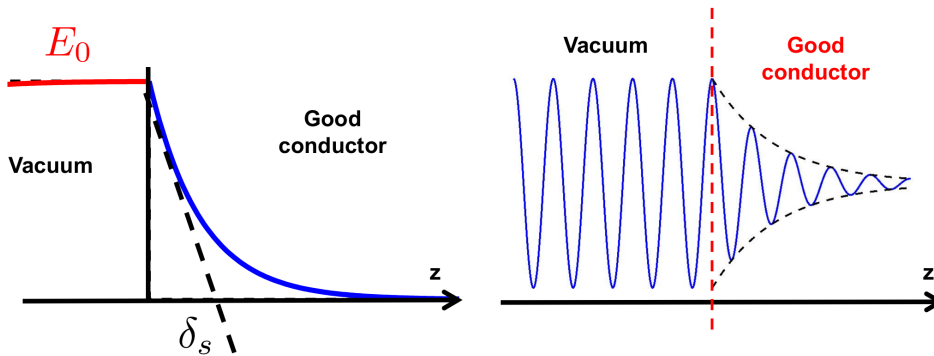


Fig. II.1.6: Exponential attenuation of the electric field entering in a lossy medium and physical meaning of the skin depth δ_S .

If a TEM plane wave impinges on a good planar conductor, the field actually entering in the conductor is very small (cancelling out for $\sigma \rightarrow 0$). Indeed most of the field is reflected back and the transmitted part is attenuated. In thickness of 5–6 skin depths the field is usually assumed negligible (e.g. $\delta_S < 1\mu$ m for copper at 10 GHz) and in practice one assumes always that the power transmitted into the conductor is dissipated as heat within a very short distance from the surface. The situation is schematically shown in Fig. II.1.7.

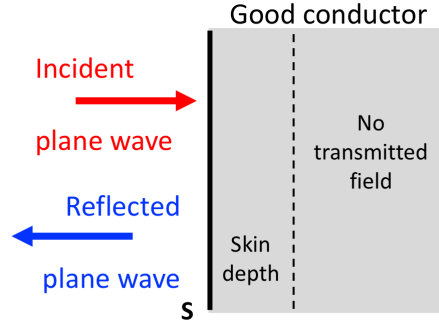


Fig. II.1.7: Surface impedance approximation to account electromagnetic field propagation in presence of good conductors.

The widely used approximation to deal with waves impinging in good conductors is called “surface impedance” approximation: the main idea is to replace the exponentially decaying current in the whole conductor volume with a uniform current extending a distance of one skin depth. The volume current \vec{J}_τ

$$\vec{J}_\tau = \begin{cases} \vec{J}_S/\delta_S & \text{if } 0 < z < \delta_S \\ 0 & \text{if } z > \delta_S \end{cases} \quad \text{being} \quad \vec{J}_S = \hat{n} \times \vec{H} \Big|_S \quad \text{when } \sigma \rightarrow \infty.$$

Applying Ohm’s law, the power loss P_t reads

$$P_t = \frac{1}{2\sigma} \int_S \int_0^{\delta_S} \frac{|\vec{J}_S|^2}{\delta_S^2} dS dz = \frac{1}{2} \frac{1}{\sigma \delta_S} \int_S |\vec{J}_S|^2 dS = \frac{R_S}{2} \int_S |\hat{n} \times \vec{H}|^2 dS, \quad (\text{II.1.35})$$

where $R_S = 1/\sigma \delta_S$ is called surface resistance.

This method is very general, applying to fields other than plane waves and to conductors of arbitrary shape, as long as bends or corners have radii on the order of a skin depth or larger. The method is also quite accurate, as the only approximation was that $\eta \ll \eta_0$, which is a good approximation. As an example, copper at 1 GHz has $|\eta| = 0.012 \Omega$, which is indeed much less than $\eta_0 = 377 \Omega$.

II.1.3 Solution of Maxwell’s equations in closed structures

II.1.3.1 General boundary value problem

A boundary value problem in microwave engineering involves finding a solution to Maxwell’s equations within a certain region of space, while satisfying prescribed boundary conditions on the surfaces that define the boundaries of that region. These boundary conditions specify how the electromagnetic fields behave at the interfaces or boundaries of the structure or device under consideration. For example, in the design of a waveguide or an antenna, the boundary conditions may specify the continuity of the tangential components of the electric and magnetic fields across the boundary, as well as the absence of electric charges or currents on the boundary surfaces.

It is common practice in the analysis of electromagnetic boundary-value problems to use auxiliary vector potentials as aids in obtaining solutions for the electric \vec{E} and magnetic \vec{H} fields. The most common vector potential functions are the \vec{A} , magnetic vector potential, and \vec{F} , electric vector potential.

They are used extensively in the solution of antenna radiation problems. Although the electric and magnetic field intensities \vec{E} and \vec{H} represent physically measurable quantities, for most engineers the vector potentials are strictly mathematical tools. The introduction of the potentials often simplifies the solution, even though it may require determination of additional functions. Much of the discussion in this section is borrowed from [1].

The Hertz vector potentials $\vec{\Pi}_e$ and $\vec{\Pi}_h$ make up another pair. The Hertz vector potential $\vec{\Pi}_e$ is analogous to \vec{A} and $\vec{\Pi}_h$ is analogous to \vec{F} , with a proportionality constant that is a function of the frequency and the constitutive parameters of the medium. In the solution of a problem, only one set, \vec{A} and \vec{F} or $\vec{\Pi}_e$ and $\vec{\Pi}_h$, is required.

The main objective of this section is to obtain electromagnetic field configurations (i.e. modes) of boundary-value propagation problems in waveguides. These field configurations must satisfy Maxwell's equations or the wave equation, as well as the appropriate boundary conditions. The procedure is to specify the electromagnetic boundary-value problem, which may or may not contain sources, and to obtain the field configurations that can exist within the region of the boundary-value problem. This can be accomplished in either of two ways, as shown in Fig. II.1.8.

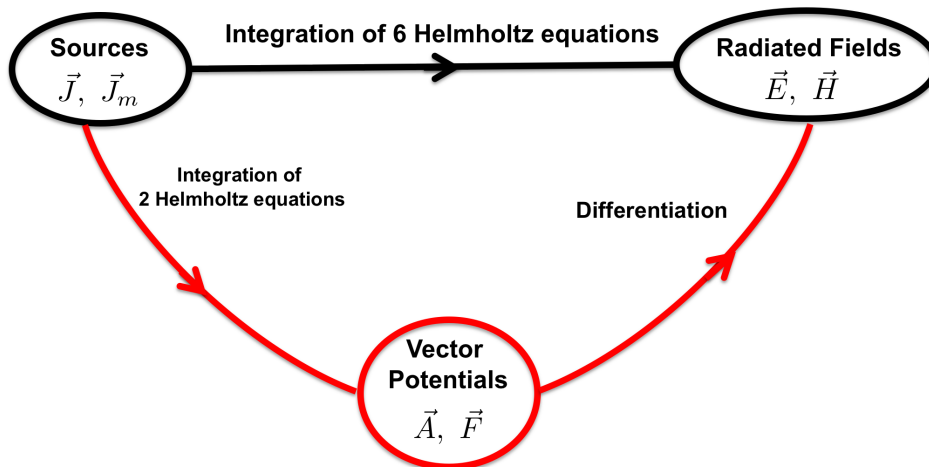


Fig. II.1.8: Block diagram for computing radiated fields from electric and magnetic sources, taken from Ref. [1].

One procedure for obtaining the electric and magnetic fields of a desired boundary-value problem is to use Maxwell's or the Helmholtz equations for the fields \vec{E}, \vec{H} . This is accomplished essentially in one step, and it is represented in Fig. II.1.8 by the black path. In a homogeneous medium, any solution for the time-harmonic electric and magnetic fields must satisfy Maxwell's equations

$$\begin{aligned}
 1. \nabla \cdot \vec{E} = \rho/\epsilon, \quad 2. \nabla \cdot \vec{H} = \rho_m/\mu, \quad 3. \nabla \times \vec{E} = -j\omega\mu\vec{H} - \vec{J}_m \quad 4. \nabla \times \vec{H} = j\omega\epsilon\vec{E} + \vec{J}
 \end{aligned}
 \tag{II.1.36}$$

or the vector Helmholtz equations

$$\begin{aligned}\nabla^2 \vec{E} + k^2 \vec{E} &= \nabla \times \vec{J}_m + j\omega\mu\vec{J} + \nabla\rho/\varepsilon \\ \nabla^2 \vec{H} + k^2 \vec{H} &= -\nabla \times \vec{J} + j\omega\varepsilon\vec{J}_m + \nabla\rho_m/\mu\end{aligned}\quad \text{being } k^2 = \omega^2\mu\varepsilon. \quad (\text{II.1.37})$$

In regions where there are no sources, $\vec{J} = \vec{J}_m = 0$ and $\rho = \rho_m = 0$. In these regions, the preceding equations are of simpler form. Whereas the electric current density \vec{J} may represent either actual or equivalent sources, the magnetic current density \vec{J}_m can only represent equivalent sources.

Although all of these equations will still be satisfied, an alternate two-step procedure is commonly used for the solution of the electric and magnetic fields using the auxiliary vector potentials, \vec{A} and \vec{F} , as shown in the red path of Fig. II.1.8. In the first step, the vector potentials \vec{A} and \vec{F} are found, once the boundary-value problem is specified; they satisfy the vector Helmholtz equations for the potentials, i.e.

$$\nabla^2 \vec{F} + k^2 \vec{F} = -\mu\vec{J}_m \quad \text{and} \quad \nabla^2 \vec{A} + k^2 \vec{A} = -\mu\vec{J} \quad \text{with} \quad k^2 = \omega^2\mu\varepsilon. \quad (\text{II.1.38})$$

In the second step, the electric and magnetic fields are found, after the vector potentials are determined. The electric and magnetic fields are functions of the vector potentials according to

$$\begin{aligned}\vec{E}_A &= -j\omega\vec{A} - (j/\omega\mu\varepsilon) \nabla (\nabla \cdot \vec{A}), & \vec{E}_F &= -(1/\varepsilon) \nabla \times \vec{F}, \\ \vec{H}_A &= (1/\mu) \nabla \times \vec{A}, & \vec{H}_F &= -j\omega\vec{F} - (j/\omega\mu\varepsilon) \nabla (\nabla \cdot \vec{F}),\end{aligned}\quad (\text{II.1.39})$$

that is

$$\vec{E} = \vec{E}_A + \vec{E}_F \quad \text{and} \quad \vec{H} = \vec{H}_A + \vec{H}_F. \quad (\text{II.1.40})$$

Although it requires two steps, it is often simpler and more straightforward and hence it is often preferred.

In electromagnetic theory, a mode refers to a specific pattern of electromagnetic fields that satisfies the boundary conditions within a given structure or device. These modes represent distinct ways in which electromagnetic energy can propagate and resonate within the system. Understanding and computing the modes in electromagnetic structures is crucial in RF problems for several reasons.

Firstly, modes provide valuable insight into how electromagnetic energy behaves within a structure or device. By computing the modes, engineers can determine the distribution of electric and magnetic fields, as well as the corresponding frequencies and propagation characteristics associated with each mode. This information is essential for optimising the performance of RF systems, such as antennas, waveguides, resonators, and transmission lines.

Secondly, modes help in analysing and designing RF components. Different modes can exhibit unique characteristics, such as varying field distributions, polarisation states, and propagation velocities. By studying the properties of each mode, engineers can tailor the design parameters of RF components to meet specific performance requirements, such as impedance matching, bandwidth, radiation pattern (in antennas) and loss reduction.

Moreover, computing the modes allows engineers to identify resonant frequencies and resonant modes within a resonant structure. Resonant modes occur when the electromagnetic energy stored in the system oscillates at a particular frequency with minimal energy losses. These resonances are crucial in

RF devices devoted to particle manipulation in accelerators. A detailed description of such devices will be subject of Chapter II.2 on RF engineering.

The rest of the section is devoted to applying the previous equations to the computation of modes in cylindrical metallic waveguides. Modes are solutions of the homogeneous equations

$$\nabla^2 \vec{F} + k^2 \vec{F} = 0 \quad \text{and} \quad \nabla^2 \vec{A} + k^2 \vec{A} = 0 \quad \text{with} \quad k^2 = \omega^2 \mu \epsilon. \quad (\text{II.1.41})$$

Equation II.1.40 implies that the modes are the superposition of modes related to the \vec{A} potential, i.e. \vec{E}_A, \vec{H}_A and modes related to the \vec{F} potential, i.e. \vec{E}_F, \vec{H}_F . By knowing them, RF designers can foresee the shape of the field inside any structure. We will see that \vec{E}_A, \vec{H}_A as well as \vec{E}_F, \vec{H}_F have peculiar properties useful in the applications to particle accelerators.

II.1.3.2 Cylindrical metallic waveguides

A cylindrical metallic microwave waveguide is a structure designed to guide and propagate electromagnetic waves at microwave frequencies. It is a hollow metal tube with a circular cross-section, and its primary purpose is to confine and control the transmission of microwave signals within its structure. Unlike free-space radiation, a waveguide ensures that microwave energy is directed from one point to another without significant loss. They also have the capability to handle high power levels without substantial degradation, making them essential in delivering high-power to accelerating or deflecting structures. Typical geometries are shown in Fig. II.1.9: a cylindrical waveguide has always one direction in which the size is much bigger than the others; this is the field propagation direction and we label it \hat{z} -direction.

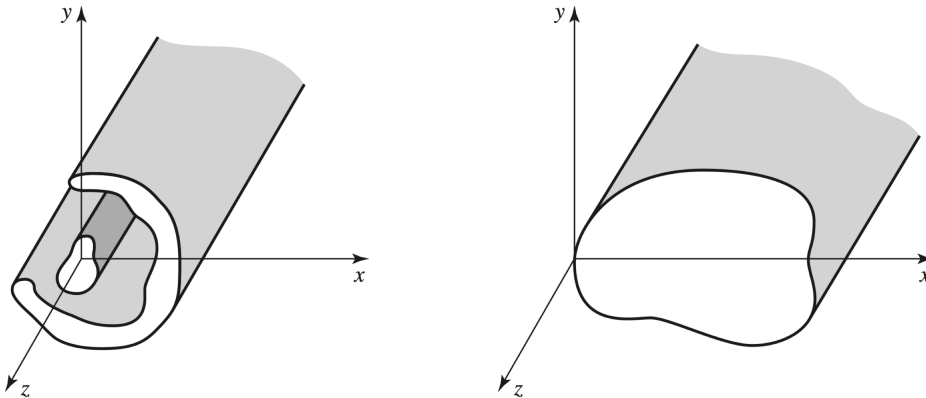


Fig. II.1.9: Cylindrical waveguides along the \hat{z} -direction, taken from Ref. [2].

Because of the symmetry, we can assume

$$\vec{A} = \hat{z} A_z(x, y) e^{-j\beta z} = \hat{z} A \quad \text{and} \quad \vec{F} = \hat{z} F_z(x, y) e^{-j\beta z} = \hat{z} F. \quad (\text{II.1.42})$$

The ∇^2 acts on the z -coordinate as well as on the transverse coordinate, i.e.

$$\nabla^2 \dots = \nabla_t^2 \dots + \frac{\partial^2}{\partial z^2} \dots, \quad (\text{II.1.43})$$

where ∇_t^2 acts on the x, y -plane orthogonal to the propagation axis. Depending on the coordinate system used to describe the problem, ∇_t^2 will have different expressions, as shown in Sec. II.1.3.3.

The two Helmholtz equations read now

$$\nabla_t^2 A_z + (k^2 - \beta^2) A_z = 0 \quad \text{and} \quad \nabla_t^2 F_z + (k^2 - \beta^2) F_z = 0; \quad (\text{II.1.44})$$

using Eq. II.1.39, written for potential with only \hat{z} component as in Eq. II.1.42, one gets

$$\vec{H}_A = \vec{h}_t e^{-j\beta z} \quad \text{and} \quad \vec{E}_A = (\vec{e}_t + \hat{z}e_z) e^{-j\beta z}. \quad (\text{II.1.45})$$

Such a field propagates in the positive \hat{z} direction, with the interesting feature of having the magnetic field always transverse to the waveguide axis or, equivalently, having only the electric field with a component on the waveguide axis (i.e. the \hat{z} axis). For this reason, the resulting mode is called Transverse Magnetic (TM) mode or E-mode.

Analogously, inserting \vec{F} from Eq. II.1.42 into Eq. II.1.39, one gets

$$\vec{H}_F = (\vec{h}_t + \hat{z}e_z) e^{-j\beta z} \quad \text{and} \quad \vec{E}_F = \vec{e}_t e^{-j\beta z}, \quad (\text{II.1.46})$$

which is a field propagating in the positive \hat{z} direction having the electric field always transverse to the waveguide axis or, equivalently, having only the magnetic field with a component on the waveguide axis (i.e. the \hat{z} axis). For this reason, the resulting mode is called Transverse Electric (TE) mode or H-mode.

To conclude, Eq. II.1.40 is telling us that any propagating field in the waveguide is a superposition of fields having a magnetic field transverse to the waveguide axis (TM modes) and fields having electric the field transverse to the waveguide axis (TE modes).

Modes in a waveguide are solutions of the homogeneous equations, i.e. they are a complete set for the solutions of the eigenvalue problem, thus any field existing in the waveguide is a superposition of those modes. Moreover those modes can propagate independently, one from the other, that is we could, in principle, excite them independently.

II.1.3.2.1 Example: TEM waves in metallic waveguides

We now look for the possibility of having a Transverse Electric Magnetic (TEM) mode, i.e. a mode being simultaneously TE and TM, as is the plane wave in free space seen in Sec. II.1.1.5.

We can look for the condition needed for a TM mode (vector potential \vec{A} , $H_z = 0$) for having also $E_z = 0$. Considering \vec{A} as in Eq. II.1.42, we can write

$$\nabla \cdot \vec{A} = -j\beta A_z e^{-j\beta z} \quad \rightarrow \quad \vec{E}_A = -\frac{j}{\omega\mu\epsilon} (\omega^2\mu\epsilon - \beta^2) A_z e^{-j\beta z} \hat{z} - \frac{\beta}{\omega\mu\epsilon} \nabla_t A_z e^{-j\beta z}. \quad (\text{II.1.47})$$

Then if $\beta^2 = \omega^2 \mu \epsilon = k^2$, e_z is vanishing and the field becomes

$$\vec{E} = -\frac{1}{\sqrt{\mu\epsilon}} \nabla_t A_z e^{-j\omega\sqrt{\mu\epsilon}z} \quad \vec{H} = \frac{1}{\mu} \nabla_t \times (\hat{z} A_z) e^{-j\omega\sqrt{\mu\epsilon}z}. \quad (\text{II.1.48})$$

Moreover A_z satisfies the Laplace equation, as for static scalar potential V in Eq. II.1.4, since

$$\nabla_t^2 A_z = -(k^2 - \beta^2) A_z = 0.$$

The electric field is the ∇_t of a solution of a Laplace equation, therefore it has transversely the same “shape” as an electrostatic field even if is propagating in the \hat{z} -direction at $v_p = 1/\sqrt{\mu\epsilon}$, that is the speed of light, as stated by the $\exp(-j\omega\sqrt{\mu\epsilon}z)$ term.

In conclusion, a TEM wave in metallic waveguides is possible if there are at least two conductors. It can be computed by considering the electrostatic boundary value problem (i.e. including the boundary conditions) to get \vec{e}_t , then

$$\vec{h}_t = \sqrt{\frac{\epsilon}{\mu}} \hat{z} \times \vec{e}_t = \frac{1}{Z_{\text{TEM}}} \hat{z} \times \vec{e}_t \quad \text{and} \quad \vec{E} = \vec{e}_t e^{-j\omega\sqrt{\mu\epsilon}z}, \quad \vec{H} = \vec{h}_t e^{-j\omega\sqrt{\mu\epsilon}z}. \quad (\text{II.1.49})$$

TEM waves are synchronous with relativistic particles, since they propagate with a phase velocity equal to the speed of light, but unfortunately they can not be used directly to accelerate particles, since the electric field is transverse to the propagation direction. Nevertheless Fig. II.1.10 shows an example of a strip-line waveguide used in beam position monitor in a high brightness LINAC. The signal excited by the beam is “guided” away by the strip towards a detector.

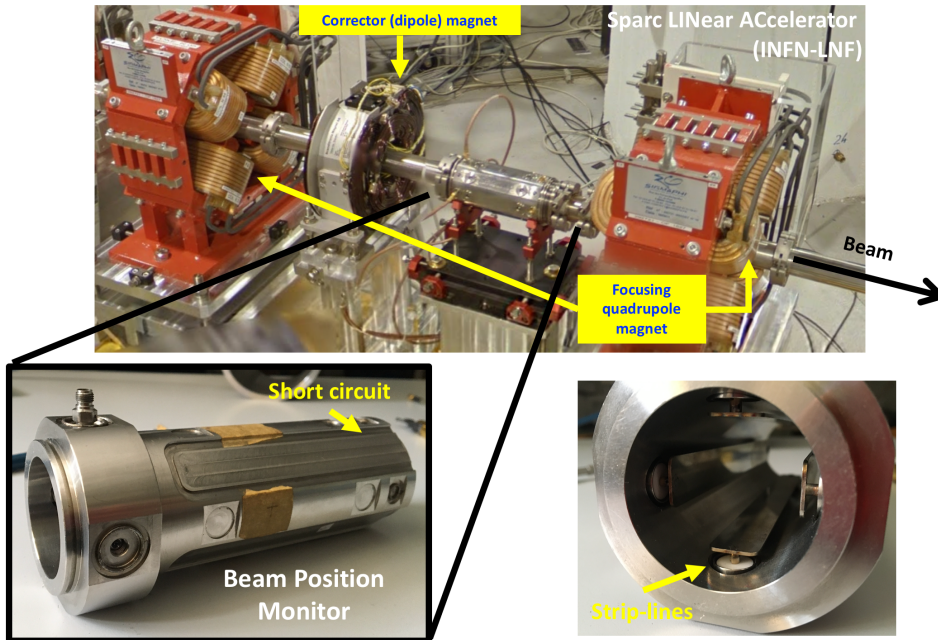


Fig. II.1.10: TEM waveguides: strip-line Beam Position Monitor in SPARC high brightness LINAC [11].

II.1.3.3 General solution for fields in cylindrical waveguides

The potentials satisfy the Helmholtz equations in the transverse coordinates

$$\nabla_t^2 A_z + k_t^2 A_z = 0 \quad \nabla_t^2 F_z + k_t^2 F_z = 0 \quad \text{with} \quad k_t^2 = k^2 - \omega^2 \mu \varepsilon, \quad \varepsilon = \varepsilon_0 \varepsilon_r (1 - j \tan \delta); \quad (\text{II.1.50})$$

the A_z equation refers to TM-modes, while the solution of the F_z equation are the TE-modes.

Figure II.1.11 defines the coordinate systems in two very common cylindrical waveguides, the rectangular cross-section and the circular cross-section ones. According to such coordinates, one can write the Laplacian operator

$$\nabla_t^2 = \frac{\partial^2}{\partial x^2} + \frac{\partial^2}{\partial y^2} \quad \text{and} \quad \nabla_t^2 = \frac{\partial^2}{\partial \rho^2} + \frac{1}{\rho} \frac{\partial}{\partial \rho} + \frac{1}{\rho^2} \frac{\partial^2}{\partial \phi^2} \quad (\text{II.1.51})$$

in rectangular and cylindrical coordinates respectively.

As shown in [ref. to Heino Henke], a very common way to solve Eq. II.1.50 is with the *separation of variables* technique, i.e. for example for A_z one seeks solution in the form

$$A_z(x, y) = X(x)Y(y) \quad \text{and} \quad A_z(\rho, \phi) = R(\rho)\Phi(\phi) \quad (\text{II.1.52})$$

for rectangular and cylindrical coordinates respectively. The solution of the eigenvalue problem of Eq. II.1.50 is an eigenfunction (i.e. A_z or F_z) with a corresponding eigenvalue (k_t). Then, for every eigenfunction one can compute the fields from Eq. II.1.39 and then apply the boundary conditions. Such fields are called modes and they are ordered according to two indices; each mode has a field shape and a propagation constant, i.e.

$$\vec{e}_{m,n}, \vec{h}_{m,n} \quad \text{and} \quad \beta_{m,n} = \sqrt{\omega^2 \mu \varepsilon - k_{t(m,n)}^2}. \quad (\text{II.1.53})$$

Because of the general properties of solutions of eigenvalue problems, any field in the waveguide can always be imagined as a superposition of the modes, that is

$$\vec{E} = \sum_{m,n} a_{m,n} \vec{e}_{m,n} e^{-j\beta_{m,n}z} \quad \text{and} \quad \vec{H} = \sum_{m,n} b_{m,n} \vec{h}_{m,n} e^{-j\beta_{m,n}z}. \quad (\text{II.1.54})$$

$\beta_{m,n}$ can be an imaginary or a real number, meaning that the field can propagate ($\beta_{m,n}$ real) or be attenuated ($\beta_{m,n}$ imaginary). The $a_{m,n}$, $b_{m,n}$ coefficients, i.e. the field amplitude, depend on the sources; on the contrary the shape of field depends on the modes, i.e. on the shape and on the dimensions of the waveguide.

II.1.3.3.1 Example: TE mode (H-mode) in rectangular waveguide

Transverse Electric (TE) modes can be computed from F_z using the separation of variables, thus from Eqs. II.1.50, II.1.51, II.1.52

$$F_z = X(x)Y(y) \quad \rightarrow \quad \nabla_t^2 F_z + k_t^2 F_z = YX'' + XY'' + k_t^2 XY = 0 \quad \rightarrow \quad \frac{X''}{X} + \frac{Y''}{Y} + k_t^2 = 0.$$

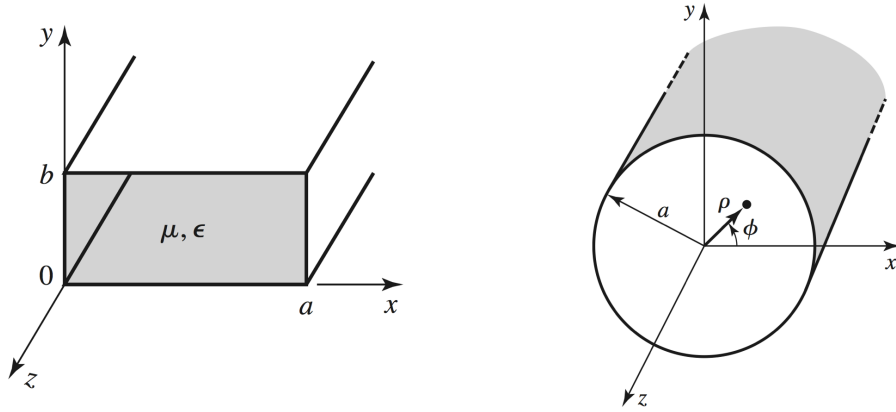


Fig. II.1.11: Rectangular and circular waveguides, taken from Ref. [2].

The last equation is a sum of three terms: the first is a function only of x , the second only of y and the third is a constant. Therefore it can be valid only if the three terms are constant themselves, i.e.

$$\frac{X''}{X} = -k_x^2, \quad \frac{Y''}{Y} = -k_y^2 \quad \text{where} \quad k_t^2 = k_x^2 + k_y^2, \quad (\text{II.1.55})$$

the last equation is called the constraint condition. The solutions of Eqs. II.1.55 are straightforward:

$$X(x) = C_1 \cos(k_x x) + D_1 \sin(k_x x) \quad \text{and} \quad Y(y) = C_2 \cos(k_y y) + D_2 \sin(k_y y),$$

being C_1, C_2, D_1, D_2 integration constants depending on the boundary conditions on the electric field which is proportional to

$$e_x = -\frac{1}{\varepsilon} \frac{\partial F_z}{\partial y} = -\frac{1}{\varepsilon} X Y' = -\frac{k_y}{\varepsilon} [C_1 \cos(k_x x) + D_1 \sin(k_x x)] [-C_2 \sin(k_y y) + D_2 \cos(k_y y)].$$

Considering the geometry in the left picture of Fig. II.1.11 and assuming a perfect conductor, the E_x must be vanishing at the bottom and top walls, thus

$$\begin{aligned} e_x(0 \leq x \leq a, y = 0) = 0 &\quad \rightarrow \quad D_2 = 0 \\ e_x(0 \leq x \leq a, y = a) = 0 &\quad \rightarrow \quad k_y b = n\pi \quad n = 0, 1, 2, \dots \end{aligned}$$

Using the same reasoning on E_y , one finds a similar condition on k_x and from the constraint condition of Eq. II.1.55, eventually we get

$$\beta_{m,n} = \sqrt{\omega^2 \mu \varepsilon - \left(\frac{m\pi}{a}\right)^2 - \left(\frac{n\pi}{b}\right)^2} \quad (\text{II.1.56})$$

which used in Eq. II.1.54 gives the field expressions.

Depending on the frequency, the propagation constant can be either a real positive number or an imaginary one. When the $\beta_{m,n}$ is real, the mode (m, n) field is propagating along \hat{z} -direction while if

$\beta_{m,n}$ is imaginary the field is exponentially decaying and the mode is referred to as an evanescent mode. The frequency at which $\beta_{m,n} = 0$ is called cutoff frequency f_c

$$(f_c)_{m,n} = \frac{1}{2\pi\sqrt{\mu\epsilon}} \sqrt{\left(\frac{m\pi}{a}\right)^2 + \left(\frac{n\pi}{b}\right)^2} \quad m, n = 0, 1, 2, \dots \quad m = n \neq 0. \quad (\text{II.1.57})$$

The mode can propagate without attenuation at frequencies above its cutoff frequency, while it is evanescent (i.e. exponentially attenuated) for frequencies smaller than its cutoff one.

The plot of the propagation constant $\beta_{m,n}$ for frequencies above the cutoff is called waveguide dispersion curve. Figure II.1.12 is the dispersion curve for the standard rectangular waveguide for X-band (called WR90). Each mode has a different dispersion curve in the plot and the name of the mode is shown in the same colour of the corresponding curve. Different modes may have identical dispersion curve, as for $\text{TE}_{1,1}$ and $\text{TM}_{1,1}$. We did not explicitly derive TM modes, i.e. modes descending from \vec{A} potential. The procedure is analogous to the previous one and details can be found in Ref. [1].

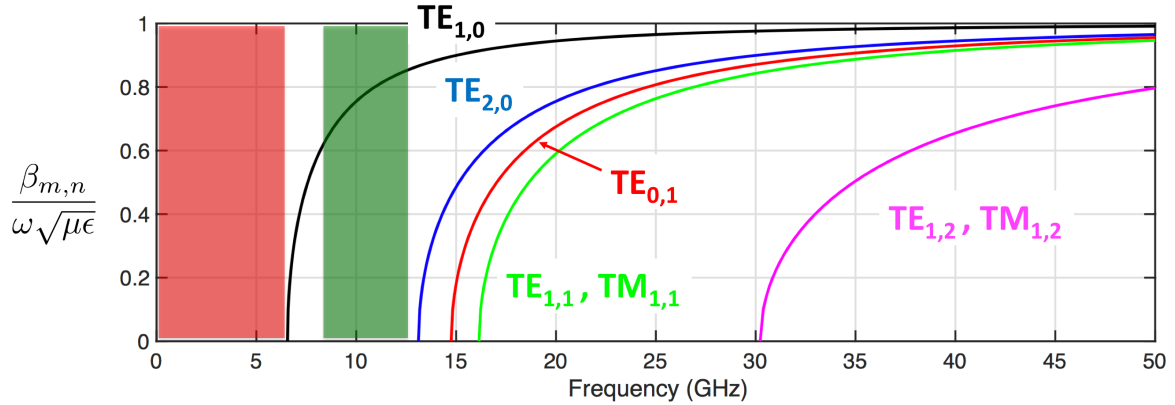


Fig. II.1.12: Dispersion diagram of the WR90 rectangular waveguide for X-band. ($a = 22.86$ mm, $b = 10.16$ mm).

The mode with the smaller cutoff frequency is called the fundamental mode; in metallic waveguides the fundamental mode is always a TE and for the rectangular waveguide is the $\text{TE}_{1,0}$. The frequencies range below the fundamental mode cutoff frequency is called waveguide cutoff region since no field can propagate in the waveguide.

The frequency range between the first and second mode cutoff frequencies is called the uni-modal propagation range since only one mode (the fundamental one) is propagating and all the others are evanescent. This is the region preferred for applications since the field properties are known, since it must be $\text{TE}_{1,0}$ mode. Actually, the frequency range used for applications is a bit smaller, typically from a frequency 25% bigger than the fundamental mode cutoff frequency to the one 5% smaller than the first high order mode cutoff frequency. Thus, according to the dispersion diagram of WR90 waveguide in Fig. II.1.12, the practically used single mode bandwidth is $1.25(f_c)_{1,0}$ to $0.95(f_c)_{2,0}$. Where the dispersion curve is vertical, it implies that slightly different frequencies may have very different propagation constants, that is phase velocity; such regions are referred to as high dispersion frequency ranges. The

white region between the red one (waveguide cutoff) and the green one (used for uni-modal propagation) is a high dispersion region for the fundamental mode and it is not used in applications even if in principle only the fundamental mode is propagating.

The transverse field pattern of a $TE_{m,n}$ mode exhibits variations along both the x and y axes of the waveguide cross-section. The electric field distribution typically varies sinusoidally along each axis, with m and n representing the number of half periods or maxima/minima along the respective axes. In general, for a $TE_{m,n}$ mode, the transverse field pattern can be visualised as having m maxima or minima along the x -axis and n maxima or minima along the y -axis within the waveguide cross-section. The specific distribution of electric field maxima and minima along these axes depends on the mode order and the geometry of the waveguide. Figure II.1.13 shows the most common ones, namely the lower order ones: for TE-modes (TM-modes) electric (magnetic) field component is shown. To understand which field is shown, reader should recall that those plots are usually done for perfectly conducting walls; therefore electric field \vec{E} is always perpendicular to the walls while \vec{H} is tangential.

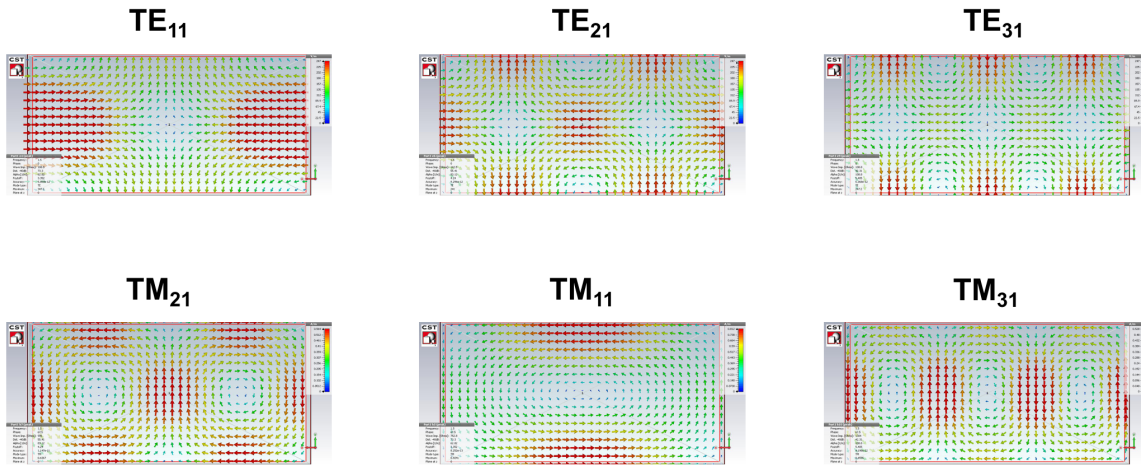


Fig. II.1.13: Electric field for TE modes and magnetic field for TM modes in the rectangular waveguide on a generic cross section of a the waveguide. (CST simulation [12], courtesy of L. Ficcadenti).

II.1.3.4 Modes impedance and propagation constant

The solution of Maxwell's equations for a given problem is complete, giving electric and magnetic fields at all points in the space. Usually we are interested in voltages or currents at a set of terminals and/or power flow, and not in fields at all points of the space.

One typical problem to be solved is the study and characterisation of microwave circuits and components within a larger network through microwave network analysis. To this extent transmission line models are often used, thus considering each mode of the waveguide as a transmission line with its own properties, which are frequency dependent. For instance the propagation constant is

$$\beta_{m,n} = \sqrt{\omega^2 \mu \epsilon - k_t^2(m,n)}, \quad (\text{II.1.58})$$

while the impedance differs for $TE_{m,n}$ and $TM_{m,n}$ modes according to

$$\begin{aligned} Z_{m,n}^{TE} &= \frac{e_{x,m,n}}{h_{y,m,n}} = \frac{-e_{y,m,n}}{h_{x,m,n}} = \frac{\omega\mu}{\beta_{m,n}} = \eta \frac{k}{\beta_{m,n}}, \\ Z_{m,n}^{TM} &= \frac{e_{x,m,n}}{h_{y,m,n}} = \frac{-e_{y,m,n}}{h_{x,m,n}} = \frac{\beta_{m,n}}{\omega\epsilon} = \eta \frac{\beta_{m,n}}{k}. \end{aligned} \quad (\text{II.1.59})$$

For the reader's convenience, we summarise here the three different impedances that are usually used in RF engineering.

– **Intrinsic impedance of the medium**

This impedance is dependent only on the material parameters of the medium and it is equal to the wave impedance for plane waves.

$$\eta = \sqrt{\frac{\mu}{\epsilon}} \quad \text{and} \quad \eta_0 = \sqrt{\frac{\mu_0}{\epsilon_0}} = 377\Omega.$$

– **Wave impedance**

This impedance is a characteristic of the particular type of wave. TEM, TM, and TE waves each have different wave impedance (Z^{TEM} , Z^{TM} , Z^{TE}), which may depend on the type of guide, the material, and the operating frequency. Sometimes one uses also its inverse, called admittance.

$$Z_{\text{wave}} = \frac{e_t}{h_t} = \frac{1}{Y_{\text{wave}}}.$$

– **Characteristic impedance**

The characteristic impedance is the ratio of voltage to current for a travelling wave on a transmission line. Because voltage and current are uniquely defined for TEM waves, the characteristic impedance of a TEM wave is unique. TE and TM waves, however, do not have uniquely defined voltages and currents, so the characteristic impedance for such waves may be defined in different ways.

$$Z_0 = \frac{1}{Y_0} = \frac{V^+}{I^+}.$$

II.1.4 Exercises

II.1.4.1 Single mode operation of a commercial rectangular waveguide

II.1.4.1.1 Question

A WR90 waveguide, also known as WG16 in Europe, is a standard rectangular waveguide that is widely used in microwave and millimeter-wave technology. The “WR” stands for “Waveguide Rectangular” and the number “90” indicates the internal width of the waveguide in hundredths of an inch. Specifically, the WR90 waveguide has internal dimensions of 0.9 inches (22.86 mm) in width and 0.4 inches (10.16 mm) in height. The WR90 waveguide is engineered to operate effectively within the frequency range of 8.2 GHz to 12.4 GHz, used in state-of-the-art X-band accelerating structures. Its dispersion diagram was given in Fig. II.1.12.

Labelling the longest side of the waveguide cross-section as a and the shortest one as b , as done in the rectangular waveguide shown in Fig. II.1.11, find the smallest ratio a/b allowing the largest bandwidth of single mode operation. Moreover, defining the single mode bandwidth as done in the text, i.e.

$$1.25 (f_c)_{1,0} < f < 0.95 (f_c)_{2,0},$$

find the single mode bandwidth for WR90 waveguide.

II.1.4.1.2 Solution

The cutoff frequencies f_c for TE-modes of a rectangular waveguide are given by Eq. II.1.57 and they are marked on the frequency axis in Fig. II.1.14. The fundamental mode $TE_{1,0}$ has the cutoff frequency $(f_c)_{1,0}$ while the position of the cutoff frequency $(f_c)_{0,1}$ depends on the value of b , that is the shortest side of the cross section. Since the position of $(f_c)_{2,0}$ is fixed, the largest bandwidth of single mode operation happens to be when $(f_c)_{0,1} = (f_c)_{2,0}$, that is $a/b = 2$. It explains why most of the commercially available rectangular waveguides are designed with $a/b \approx 2$.

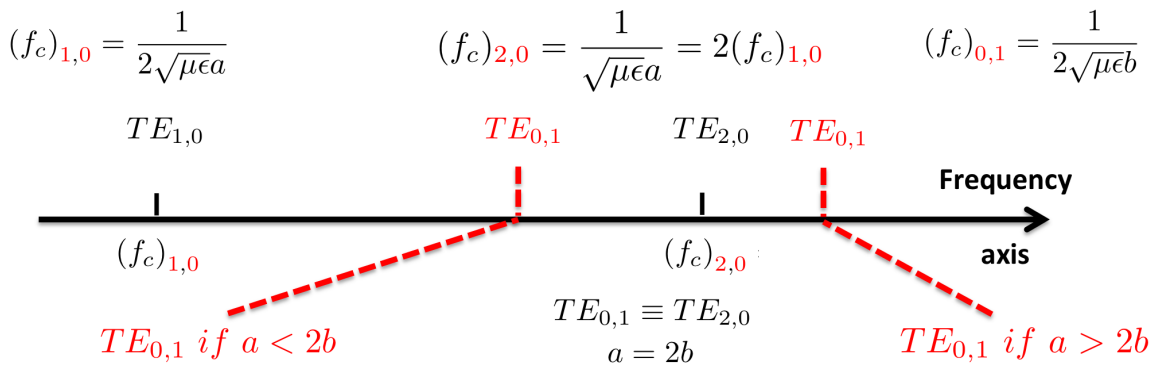


Fig. II.1.14: Cutoff frequencies of the TE modes of a rectangular waveguide in Fig. II.1.11. The cutoff frequency of the second mode (red line) depends on the geometry and it can be either a $TE_{0,1}$ or a $TE_{2,0}$. The upper formulae remind the cutoff frequencies of the $TE_{1,0}$, $TE_{2,0}$ and $TE_{0,1}$ modes respectively.

Because of the sizes, i.e. $b > 2a$, the first two cutoff frequencies are $TE_{1,0}$ and $TE_{2,0}$ with

$$(f_c)_{1,0} = c/2a = 6.56 \text{ GHz} \quad \text{and} \quad (f_c)_{2,0} = c/a = 13.11 \text{ GHz},$$

and the single mode operation bandwidth, as for instance specified by the vendors, is

$$1.25 (f_c)_{1,0} = 8.20 < f < 12.46 \text{ GHz} = 0.95 (f_c)_{2,0}.$$

II.1.4.2 Field pattern of the fundamental mode in a rectangular waveguide

II.1.4.2.1 Question

Compute the expression for the TE fields and draw the field pattern of the fundamental mode of a rectangular waveguide. Try to sketch the field of the mid-plane of a waveguide with length equal to $3\lambda/2$. Sketch also the Poynting vector $\vec{S}(\vec{r}, t)$ as defined in Eq. II.1.20.

II.1.4.2.2 Solution

The $TE_{m,n}$ modes propagating in the positive z direction have m (n) half periods (or maxima/minima) along the x (y) axis in the cross-section. Applying the solution method discussed in the text, the fields of the modes are

$$\begin{aligned} E_x^{+, (m,n)} &= a_{m,n} \frac{n\pi}{\epsilon b} \cos\left(\frac{m\pi}{a}x\right) \sin\left(\frac{n\pi}{b}y\right) e^{-j\beta_{m,n}z}, \\ E_y^{+, (m,n)} &= -a_{m,n} \frac{m\pi}{\epsilon a} \sin\left(\frac{m\pi}{a}x\right) \cos\left(\frac{n\pi}{b}y\right) e^{-j\beta_{m,n}z}, \\ E_z^{+, (m,n)} &= 0, \\ H_x^{+, (m,n)} &= a_{m,n} \frac{m\pi}{\epsilon a} \frac{\beta_{m,n}}{\omega\mu\epsilon} \sin\left(\frac{m\pi}{a}x\right) \cos\left(\frac{n\pi}{b}y\right) e^{-j\beta_{m,n}z}, \\ H_y^{+, (m,n)} &= a_{m,n} \frac{n\pi}{\epsilon b} \frac{\beta_{m,n}}{\omega\mu\epsilon} \cos\left(\frac{m\pi}{a}x\right) \sin\left(\frac{n\pi}{b}y\right) e^{-j\beta_{m,n}z}, \\ H_z^{+, (m,n)} &= -ja_{m,n} \frac{k_t^2}{\omega\mu\epsilon} \cos\left(\frac{m\pi}{a}x\right) \cos\left(\frac{n\pi}{b}y\right) e^{-j\beta_{m,n}z}. \end{aligned}$$

The fundamental mode field, i.e. for $m=1$ and $n=0$, are depicted in Fig. II.1.15, where it is clear that the boundary condition of a null tangential electric field on the waveguide surfaces is satisfied.

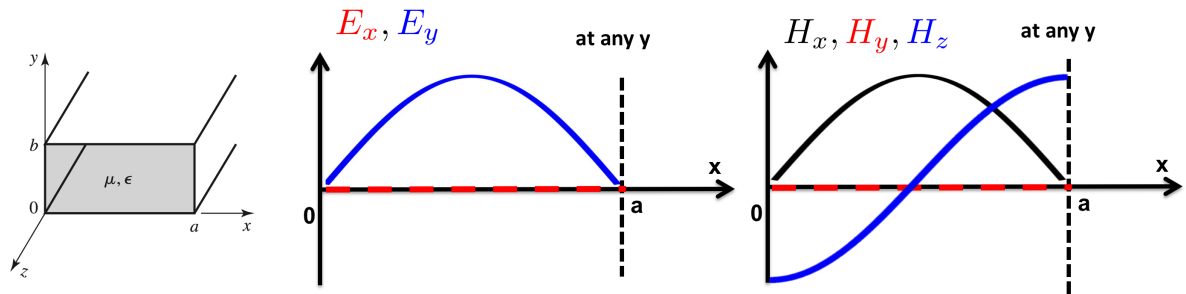


Fig. II.1.15: Field distribution of the $TE_{1,0}$ mode according to the geometry of the left picture. For clarity, we have omitted E_z , as it is zero in a TE mode.

The electric and magnetic 3D field pattern in the mid-plane of the waveguide is shown in Fig. II.1.16 for a structure $3\lambda/2$ long. The reader can find the behaviour expected from the formulae of $TE_{1,0}$ fields.

The Poynting vector of Eq. II.1.20 at a fixed time along the waveguide symmetry plane is shown in the top left picture of Fig. II.1.17. The power flowing through a surface is the flux of the Poynting Vector over that surface. The right top picture of Fig. II.1.17 shows the time average over a period of $\vec{S}(\vec{r}, t)$; it is evident that the direction of the power flow is along the z -axis and the power value (i.e. the flux of \vec{S}) is constant. It is important noticing that, according to our definition, the time average over one period is the real part of the phasor of the Poynting vector $\vec{S}(\vec{r}, \omega)$ of Eq. II.1.21. The left bottom picture of Fig. II.1.17 shows the second term of Eq. II.1.20; it contributes to the instantaneous value of the Poynting vector, but not on its time average over one period. The right bottom picture of Fig. II.1.17 shows the imaginary part of $\vec{S}(\vec{r}, \omega)$. The flux of this term along the cross section is null, meaning that it is not associated to the power flowing and it thus accounts for reactive power.

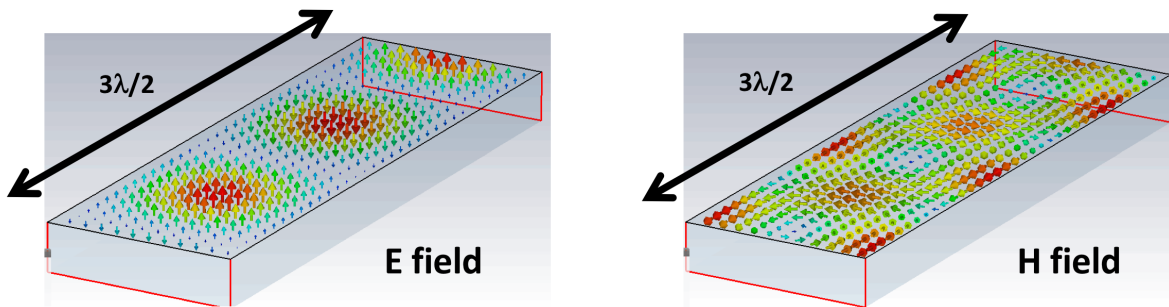


Fig. II.1.16: Electric (left plot) and magnetic field (right plot) of the $TE_{1,0}$ in the rectangular waveguide. The length of the simulated structure is $3\lambda/2$. (CST simulation [12], courtesy of L. Ficcadenti).

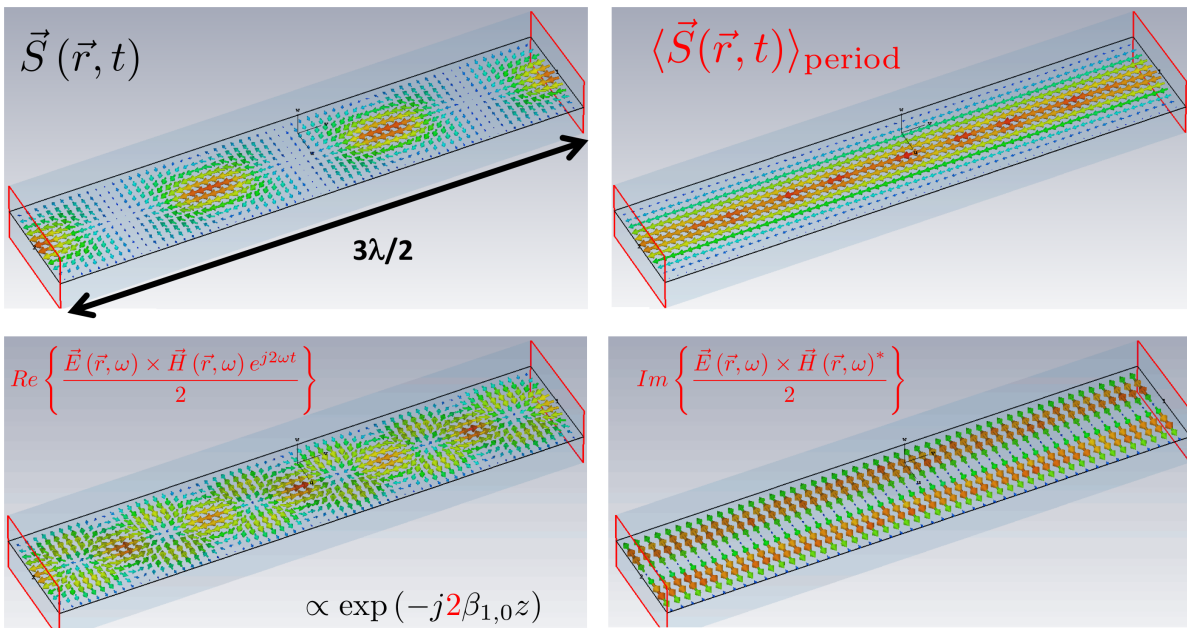


Fig. II.1.17: Poynting vector \vec{S} of the $TE_{1,0}$ in the rectangular waveguide. The length of the simulated structure is $3\lambda/2$. The left top plot is \vec{S} at a fixed time along the waveguide symmetry plane. The average of \vec{S} on one period is the right top plot. The bottom plots are respectively the $2\omega t$ oscillating part and the imaginary part of the phasor of the Poynting vector. (CST simulation [12]).

References

- [1] C.A. Balanis, *Advanced engineering electromagnetics* 2nd Edition, John Wiley & Sons, 2012, ISBN 978-0-470-58948-9, [Link](#).
- [2] D.M. Pozar, *Microwave Engineering* 4th Edition, John Wiley & Sons, 2011, ISBN 978-0-470-63155-3, [Link](#).
- [3] F. Amman *et al.*, ADONE-The Frascati 1.5 GeV electron positron storage ring, LNF-65-026, (LNF, Frascati, 1965), [Link](#).
- [4] T.P. Wangler, *RF Linear Accelerators* 2nd Edition, John Wiley & Sons, 2008, ISBN: 978-3-527-40680-7, [doi:10.1002/9783527623426](https://doi.org/10.1002/9783527623426).
- [5] B. Aune *et al.*, *Phys. Rev. ST Accel. Beams* **3** (2000) 092001, [doi:10.1103/PhysRevSTAB.3.092001](https://doi.org/10.1103/PhysRevSTAB.3.092001).
- [6] D. Alesini *et al.*, *Phys. Rev. ST Accel. Beams* **18** (2015) 092001, [doi:10.1103/PhysRevSTAB.18.092001](https://doi.org/10.1103/PhysRevSTAB.18.092001).
- [7] M. Dal Forno *et al.*, *Phys. Rev. ST Accel. Beams* **19** (2016) 011301, [doi:10.1103/PhysRevAccelBeams.19.011301](https://doi.org/10.1103/PhysRevAccelBeams.19.011301).
- [8] E. Nanni *et al.*, *Nat. Commun.* **6** (2015) 8486, [doi:10.1038/ncomms9486](https://doi.org/10.1038/ncomms9486).
- [9] T. Plettner *et al.*, *Phys. Rev. ST Accel. Beams* **9** (2006) 111301, [doi:10.1103/PhysRevSTAB.9.111301](https://doi.org/10.1103/PhysRevSTAB.9.111301).
- [10] R. E. Collin, *Field Theory of Guided Waves*, McGraw-Hill, New York, 1960.
- [11] M. Ferrario *et al.*, *Nucl. Instrum. Methods Phys. Res. B* **309** (2013) 183–188, [doi:10.1016/j.nimb.2013.03.049](https://doi.org/10.1016/j.nimb.2013.03.049).
- [12] [CST Studio Suite](#).